

Evaluations of NO_x and highly reactive VOC emission inventories in Texas and their implications for ozone plume simulations during the Texas Air Quality Study 2006

S.-W. Kim^{1,2}, S. A. McKeen^{1,2}, G. J. Frost^{1,2}, S.-H. Lee^{1,2}, M. Trainer², A. Richter³, W. M. Angevine^{1,2}, E. Atlas⁴, L. Bianco^{1,2}, K. F. Boersma^{5,6}, J. Brioude^{1,2}, J. P. Burrows^{3,7}, J. de Gouw^{1,2}, A. Fried⁸, J. Gleason⁹, A. Hilboll³, J. Mellqvist¹⁰, J. Peischl^{1,2}, D. Richter⁸, C. Rivera^{10,*}, T. Ryerson², S. te Lintel Hekkert¹¹, J. Walega⁸, C. Warneke^{1,2}, P. Weibring⁸, and E. Williams^{1,2}

¹Cooperative Institute for Research in Environmental Sciences, University of Colorado, Boulder, CO 80309, USA

²NOAA Earth System Research Laboratory, Boulder, CO 80305, USA

³Institute of Environmental Physics, University of Bremen, Germany

⁴Rosenstiel School of Marine and Atmospheric Science, Division of Atmospheric and Marine Chemistry, University of Miami, Miami, FL 33149, USA

⁵Royal Netherlands Meteorological Institute (KNMI), De Bilt, The Netherlands

⁶Eindhoven University of Technology, Eindhoven, The Netherlands

⁷Center for Ecology and Hydrology, Maclean Building, Benson Lane, Crowmarsh Gifford, 16 Wallingford, Oxfordshire, OX10 8BB, UK

⁸NCAR, Earth Observing Laboratory, Boulder, CO 80307, USA

⁹NASA Goddard Space Flight Center, Laboratory for Atmosphere, Greenbelt, MD 20771, USA

¹⁰Earth and Space Science, Chalmers University of Technology, Gothenburg, Sweden

¹¹Sensor Sense, Nijmegen, The Netherlands

* now at: Centro de Ciencias de la Atmósfera, Universidad Nacional Autónoma de México, México

Received: 20 July 2011 – Published in Atmos. Chem. Phys. Discuss.: 27 July 2011

Revised: 25 October 2011 – Accepted: 27 October 2011 – Published: 16 November 2011

Abstract. Satellite and aircraft observations made during the 2006 Texas Air Quality Study (TexAQS) detected strong urban, industrial and power plant plumes in Texas. We simulated these plumes using the Weather Research and Forecasting-Chemistry (WRF-Chem) model with input from the US EPA's 2005 National Emission Inventory (NEI-2005), in order to evaluate emissions of nitrogen oxides (NO_x = NO + NO₂) and volatile organic compounds (VOCs) in the cities of Houston and Dallas-Fort Worth. We compared the model results with satellite retrievals of tropospheric nitrogen dioxide (NO₂) columns and airborne in-situ observations of several trace gases including NO_x and a number of VOCs. The model and satellite NO₂ columns agree well for regions with large power plants and for urban areas that are dominated by mobile sources, such as Dallas. How-

ever, in Houston, where significant mobile, industrial, and in-port marine vessel sources contribute to NO_x emissions, the model NO₂ columns are approximately 50%–70% higher than the satellite columns. Similar conclusions are drawn from comparisons of the model results with the TexAQS 2006 aircraft observations in Dallas and Houston. For Dallas plumes, the model-simulated NO₂ showed good agreement with the aircraft observations. In contrast, the model-simulated NO₂ is ~60% higher than the aircraft observations in the Houston plumes. Further analysis indicates that the NEI-2005 NO_x emissions over the Houston Ship Channel area are overestimated while the urban Houston NO_x emissions are reasonably represented. The comparisons of model and aircraft observations confirm that highly reactive VOC emissions originating from industrial sources in Houston are underestimated in NEI-2005. The update of VOC emissions based on Solar Occultation Flux measurements during the field campaign leads to improved model simulations of ethylene, propylene, and formaldehyde. Reducing



Correspondence to: S.-W. Kim
(siwan.kim@noaa.gov)

NO_x emissions in the Houston Ship Channel and increasing highly reactive VOC emissions from the point sources in Houston improve the model's capability of simulating ozone (O₃) plumes observed by the NOAA WP-3D aircraft, although the deficiencies in the model O₃ simulations indicate that many challenges remain for a full understanding of the O₃ formation mechanisms in Houston.

1 Introduction

Texas is the second most populous state in the US, according to 2000 and 2010 Census data (<http://factfinder2.census.gov>). In addition to large cities, such as Houston, Dallas-Fort Worth, San Antonio, Austin, and El Paso, and numerous fossil-fueled electricity-generating power plants, one of the world's largest petrochemical complexes is located in the Houston metropolitan area, leading to complicated air quality problems in Texas and in Houston, in particular. One of the major pollutants responsible for long-standing air quality issues in Texas is ozone (O₃). Ozone, which is strongly enhanced during photochemical smog events, is a regulated pollutant, and US Environment Protection Agency (EPA) ozone standards have consistently been violated in the Houston-Galveston area for decades (<http://www.tceq.texas.gov/airquality/sip/>).

Ozone in the troposphere is produced by the oxidation of volatile organic compounds (VOCs) with nitrogen oxides (NO_x, the sum of nitrogen oxide, NO, and nitrogen dioxide, NO₂) acting as a catalyst (Haagen-Smit, 1952). Therefore, to understand the formation of ozone in the troposphere, it is essential to have accurate knowledge about its precursors, NO_x and VOCs. Mobile sources in urban areas and coal-burning power plants have been recognized as large sources of NO_x (Ryerson et al., 1998; Kim et al., 2006; Bishop and Stedman, 2008; Dallmann and Harley, 2010; Peischl et al., 2010). In Texas, in addition to these two major NO_x sources, petrochemical refineries and related industrial activities in the Houston-Galveston metropolitan area have been shown to emit large amounts of NO_x (Ryerson et al., 2003; Rivera et al., 2010; Washenfelder et al., 2010). The petrochemical facilities in this area emit high levels of very reactive VOCs, and the magnitude of reactive VOC emissions is significantly higher than predicted by inventories (Kleinman et al., 2002; Ryerson et al., 2003; Wert et al., 2003; Jiang and Fast, 2004; Jobson et al., 2004; Zhang et al., 2004; Kim et al., 2005; Murphy and Allen, 2005; Nam et al., 2006; Byun et al., 2007; Webster et al., 2007; Vizuete et al., 2008; de Gouw et al., 2009; Gilman et al., 2009; McKeen et al., 2009; McCoy et al., 2010; Washenfelder et al., 2010). A primary objective of the measurements made during the Texas Air Quality Studies in 2000 and 2006 (TexAQS 2000 and 2006) was to identify NO_x and VOC emission sources and understand their roles in ozone pollution in Texas (Parrish et al., 2009).

Our study is motivated by the need to understand NO_x and VOC emissions in Texas, with a focus on the Houston-Galveston area for the period of TexAQS 2006. Specifically, we evaluate NO_x and VOC emissions in the EPA NEI-2005 using regional model simulation results together with satellite and aircraft observations during TexAQS 2006. The manuscript is organized as follows. In Sects. 2 and 3, the model set-up and the observational data used in this study are described. The results in Sect. 4 start with the evaluation of the NO_x emission inventory through a comparison of the model tropospheric NO₂ vertical columns with satellite-retrieved columns. The NO_x emission inventory is then evaluated by comparing the model simulation of NO₂ with aircraft observations. Because the satellite-retrieved NO₂ columns have uncertainties caused by the application of an air mass factor (Boersma et al., 2004; Kim et al., 2009; Lamsal et al., 2010; Heckel et al., 2011), more definitive conclusions regarding the emission inventory are obtained using other independent observational data sets (e.g., aircraft measurements). Next, the emissions of very reactive VOCs in NEI-2005 are compared with the estimates by Solar Occultation Flux (SOF) measurements (Mellqvist et al., 2010). Ethylene and propylene emissions in the NEI-2005 are updated following the SOF observations in Mellqvist et al. (2010). Finally, the model simulations of ozone plumes with the default NEI-2005 and with updated emissions based on the findings in this study are compared with the aircraft observations, and the importance of the updated emissions in the ozone plume simulations is discussed.

2 Model simulations

2.1 Model set-up

The Weather Research and Forecasting-Chemistry (WRF-Chem) model is based on a three-dimensional, compressible, and non-hydrostatic mesoscale numerical weather prediction model, the WRF community model, developed at the National Center for Atmospheric Research in collaboration with several research institutes (Skamarock et al., 2008). The WRF-Chem model system is "online" in the sense that all processes affecting the gas phase and aerosol species are calculated in lock step with the meteorological dynamics (Grell et al., 2005). The WRF-Chem version 3.1 released on April 2009 is used in this study.

A mother and a nested domain were constructed for the simulations. The mother domain had 246 × 164 grid cells with a horizontal resolution of 20 km covering the United States (see Fig. 1 in Lee et al., 2011a). The nested domain (Fig. 1) had 226 × 231 grids with 4 km horizontal grid spacing covering the Houston-Galveston and Dallas-Fort Worth area in Texas. The horizontal grid resolution of the mother domain is appropriate for the comparisons with the satellite data and the nested domain is designed for the comparison

with the aircraft observations. The vertical grid was composed of 35 full sigma levels stretching from near surface at about 20 m (the first half sigma level) to the model top (50 hPa). The National Centers for Environmental Prediction (NCEP) Global Forecast System (GFS) model analysis data with a horizontal resolution of $1^\circ \times 1^\circ$ were used as meteorological initial and boundary conditions. The physical parameterizations used in this study were the same as in Lee et al. (2011a), which utilized an urban canopy model within the WRF model and showed excellent model performance in the Houston-Galveston area. The options relevant to chemistry, including chemical initial and boundary conditions and chemical mechanism, were the same as in Kim et al. (2009). The physical and chemical options and the anthropogenic and biogenic emission inventories used in this study are summarized in Table 1. The fine-resolution application of the WRF-Chem model to a case during the 2004 ICARTT (International Consortium for Atmospheric Research on Transport and Transformation) field campaign proved the model's capability to simulate the emissions, transport, and transformation of urban plumes originating from New York City (Lee et al., 2011b).

The WRF-Chem model used in this study does not include the NO_x emissions from lightning processes. The lightning NO_x sources missing in the model may add uncertainties in the simulated NO₂ columns (e.g., Huijnen et al., 2010). In this study, however, the NO_x emissions from large anthropogenic sources in Texas are approximately factor of 10 larger than lightning NO_x emissions (O. R. Cooper, personal communication, 2011 based on Cooper et al., 2009) and more than 50 % error in those anthropogenic emissions are focused.

The simulations were conducted from 26 July 2006 to 6 October 2006 covering the TexAQS-2006 period with a one-way nesting technique (Skamarock et al., 2008). Various modified emission inventories were tested with the default NEI-2005 as a reference. The details are summarized in the next sub-section.

2.2 Emission inventory

The reference emission inventory (NEI05-REF) used for the model simulations was based on the US EPA NEI-2005 (US EPA, 2010). The gridded (4-km resolution) and point source hourly emission files used in this study are available electronically at ftp://aftp.fsl.noaa.gov/divisions/taq/emissions_data_2005/, with only weekday emissions considered here. Specific details of the inventory are available in the readme.txt file that comes with the emissions data, but some background information about the inventory applies to inventory modifications discussed in the following text.

The four major source components (point, mobile on-road, mobile non-road, and area) were processed according to EPA recommendations with emissions data available from the US EPA as of October 2008. Thus, portions of the point and area

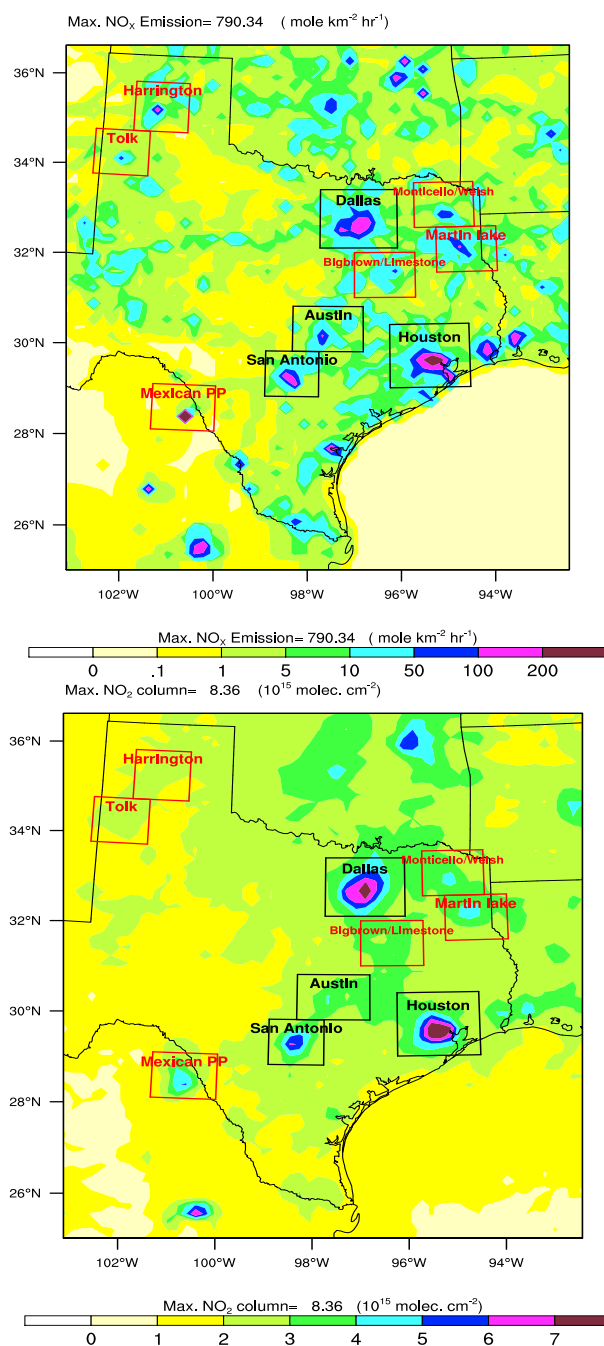


Fig. 1. Spatial distribution of NEI05-REF NO_x emissions (top) and NASA OMI NO₂ columns (bottom) in the model nested domain. The satellite columns are averaged for 26 July 2006–6 October 2006.

source emissions, updated within more recent NEI-2005 releases, were based on the earlier NEI-2002 (version 3) data (US EPA, 2008) within NEI05-REF. The point emissions included US emissions from the Continuous Emissions Monitoring System (CEMS) network for August 2006, but all other point source activity data were from the NEI-2002v3

Table 1. WRF-Chem model configuration used in this study.

Parameter	Options
Advection scheme	Positive-definite and monotonic scheme (Wang et al., 2009)
Longwave radiation	RRTM (Mlawer et al., 1997)
Shortwave radiation	Goddard shortwave scheme
Land-surface model	Noah LSM (UCM) (Chen and Dudhia, 2001; Lee et al., 2011a)
Surface layer	Similarity theory (Paulson, 1970; Dyer and Hicks, 1970)
Boundary layer scheme	YSU (Hong et al., 2006)
Cumulus parameterization	Grell-Devenyi ensemble (Grell and Devenyi, 2002)
Microphysics	Lin scheme (Lin et al., 1983)
Photolysis scheme	TUV (Madronich, 1987)
Gas phase chemistry	RACM-ESRL (Kim et al., 2009)
Aerosols	MADE (Ackermann et al., 1998), SORGAM (Schell et al., 2001)
Anthropogenic emission	EPA National Emission Inventory Year 2005
Biogenic emission	BEIS v3.13

inventory. The mobile on-road and mobile non-road US emissions were derived from EPA's National Mobile Inventory Model (NMIM) (US EPA, 2005) for July 2005. The onroad emissions were determined using the EPA's MOBILE6.2 model, and the nonroad emissions were from the NONROAD2005 model. The area emissions were based entirely on source activity data within the NEI-2002v3 inventory. NEI05-REF did not include some area sources within the more recent NEI-2005 versions, including open-ocean commercial marine vessels, off-shore oil and gas exploration and drilling sources, prescribed burning and wildfire sources. The horizontal distribution of NO_x emissions in NEI05-REF is shown in Fig. 1.

The NEI05-REF with ethylene and propylene emissions updated following Mellqvist et al. (2010), the development of which is described in Sect. 4.2.1, is denoted as NEI05-VOC. We also generated another emission inventory (NEI05-VOCNOX) from NEI05-VOC that modifies the NO_x emissions in the Houston Ship Channel area only. The NEI05-VOCNOX reduces the industrial NO_x emissions in the Houston Ship Channel by a factor of 2 and eliminates the port NO_x emissions in this region. The rationale for these modifications is given in Sect. 4.

3 Observations

3.1 Satellite retrieved NO₂ columns

The retrievals of tropospheric NO₂ columns by instruments on polar-orbiting satellites have been widely used to detect NO_x sources, derive emission trends, and evaluate existing emission inventories (e.g., Martin et al., 2003; Beirle et al., 2004; Richter et al., 2005; Kim et al., 2006; Kononov et al., 2006; van der A, 2008; Zhang et al., 2009; Kim et al., 2009; Russell et al., 2010). For the period of TexAQS

2006, the NO₂ column data are available from the SCIAMACHY (Scanning Imaging Absorption Spectrometer for Atmospheric Chartography on the EVISAT-1 satellite) and OMI (Ozone Monitoring Instrument on the Aura satellite) instruments (Bovensmann et al., 1999; Levelt et al., 2006). The satellite retrievals of tropospheric NO₂ columns have inherent uncertainties, the largest of which arise from separating the stratospheric and tropospheric contributions and from applying an air mass factor (Richter and Burrows, 2002) to convert slant columns to vertical columns (van Noije et al., 2006; Lamsal et al., 2010; Heckel et al., 2011). In order to understand uncertainties in the satellite retrievals, it is helpful to compare the data sets from various instruments and retrieval groups. In this study, we used SCIAMACHY and OMI retrievals from the University of Bremen (Kim et al., 2009) and other OMI retrievals from the Royal Netherlands Meteorological Institute (KNMI) (Boersma et al., 2004, 2007, 2011) and the US National Aeronautics and Space Administration (NASA) (NASA, 2002; Bucselo et al., 2006; Kim et al., 2009). The KNMI provided 2 OMI retrievals. The apparent differences are taken here as an indication of the inherent uncertainty in the retrieval algorithms. The satellite retrievals used in this study are standard retrievals from the 3 institutions in terms of using the NO₂ profiles from global chemical transport models. Although the WRF-Chem profiles were not used as a priori to the retrieval in this study, it will be important to test the sensitivity of the satellite retrievals over Texas to a priori model NO₂ profiles in a future study.

To systematically compare the satellite data with the model results, the WRF-Chem data are projected onto the daily orbital SCIAMACHY and OMI pixels. Because clouds inhibit the satellite from sensing the boundary layer NO₂, cloudy grid cells are filtered out. Pixels with cloud fraction <0.15 are used in the comparisons of the satellite retrievals with the model, ensuring the same number of samples in

Table 2. Evaluation of the WRF-Chem model meteorology with measurements from 10 surface stations in southeast Texas for selected days. MBE denotes mean bias error and RMSE stands for root mean square error.

Date	<i>T</i> (°C)		Wind Speed (m s ⁻¹)		Wind Direction (°)	
	MBE	RMSE	MBE	RMSE	MBE	RMSE
9/13/2006	-0.6	1.4	1.3	1.7	6.2	50.7
9/19/2006	-0.2	1.1	1.0	1.5	-7.6	22.0
9/25/2006	0.5	1.2	1.9	2.3	-2.5	18.4
9/26/2006	-1.7	2.4	1.1	1.5	-15.4	59.3
10/5/2006	-1.3	1.8	0.9	1.2	-19.0	50.9
10/6/2006	-1.7	2.3	0.8	1.2	5.9	50.2
Average for 6 days	-0.8	1.8	1.2	1.6	-5.9	44.7

each comparison. For the model and OMI satellite comparisons, only fine-resolution scenes with pixel numbers between 20 and 40 are used, so that the model ($20 \times 20 \text{ km}^2$) and satellite resolution (maximum size: $395 \text{ km}^2 \approx 30 \text{ km}$ (across track) $\times 13 \text{ km}$ (along track)) are similar.

3.2 Aircraft measurements

During the TexAQS 2006 field campaign, a NOAA WP-3D aircraft was instrumented to measure various gas- and aerosol-phase chemical species, including NO, NO₂, O₃, ethylene, propylene, and formaldehyde (HCHO) (Parrish et al., 2009). The aircraft flights were mainly targeted to sample pollution plumes within the boundary layer of eastern Texas from 31 August to 13 October 2006. The instrumentation details are described in Parrish et al. (2009). The measurements used here to study the emissions and ozone formation were from WP-3D flights on 13, 19, 25, and 26 September and 5 and 6 October 2006; all were days in which northerly flow dominated in the Houston-Galveston and Dallas-Fort Worth areas and the model performed well in terms of meteorology. The flight paths on those selected days are given in Fig. 2. Overall statistics exhibiting the model performance with respect to meteorological variables measured at surface stations and radar wind profilers for the selected days are summarized in Tables 2 and 3. The mean model biases (root mean square errors) in near-surface temperature, wind speed and wind direction relative to measurements from 10 surface stations are less than 2 °C, 2 m s⁻¹, and 20°, respectively. The comparison of the model wind speed and direction with radar wind profiler observations at the middle of the boundary layer height also shows that the mean model biases are less than $\sim 2 \text{ m s}^{-1}$ and 26°, respectively. Model boundary layer heights in comparison with those determined by radar wind profilers at Arcola and La Porte are shown in Fig. 3. At both sites, the correlation coefficient between model boundary layer height and wind profiler data is 0.87. The slopes of the linear regression between the model and profiler data in-

Table 3. Evaluation of the WRF-Chem model meteorology with wind profiler data at La Porte, Texas, for selected days. MBE denotes mean bias error and RMSE stands for root mean square error.

Date	Wind Speed (m s ⁻¹)		Wind Direction (°)	
	MBE	RMSE	MBE	RMSE
9/13/2006	1.7	2.6	15.8	40.8
9/19/2006	-0.5	2.9	-10.8	17.1
9/25/2006	1.4	1.9	-1.6	8.7
9/26/2006	2.1	2.5	-15.3	33.7
10/5/2006	1.1	1.8	-0.7	17.2
10/6/2006	1.7	2.1	-8.2	26.6
Average for 6 days	1.2	2.3	-3.3	26.3

dicating that the boundary layer heights agree within 10–20 % on average.

4 Results

4.1 Evaluation of Texas NO_x emissions

4.1.1 NO_x emission sources in Texas

In Fig. 1, boxes representing 9 regions with large NO_x emission sources in Texas and one large power plant in Mexico are overlaid on maps of the NEI05-REF emissions and of the NASA tropospheric satellite NO₂ columns averaged over the TexAQS 2006 time period. Four of these regions are cities: Dallas-Fort Worth, Houston-Galveston, Austin and San Antonio. The other source regions contain one or more electricity-generating power plants: Big Brown and Limestone, Tolk, Harrington, Monticello and Welsh, and Martin Lake. Table 4 provides detailed geographic information for the source boxes.

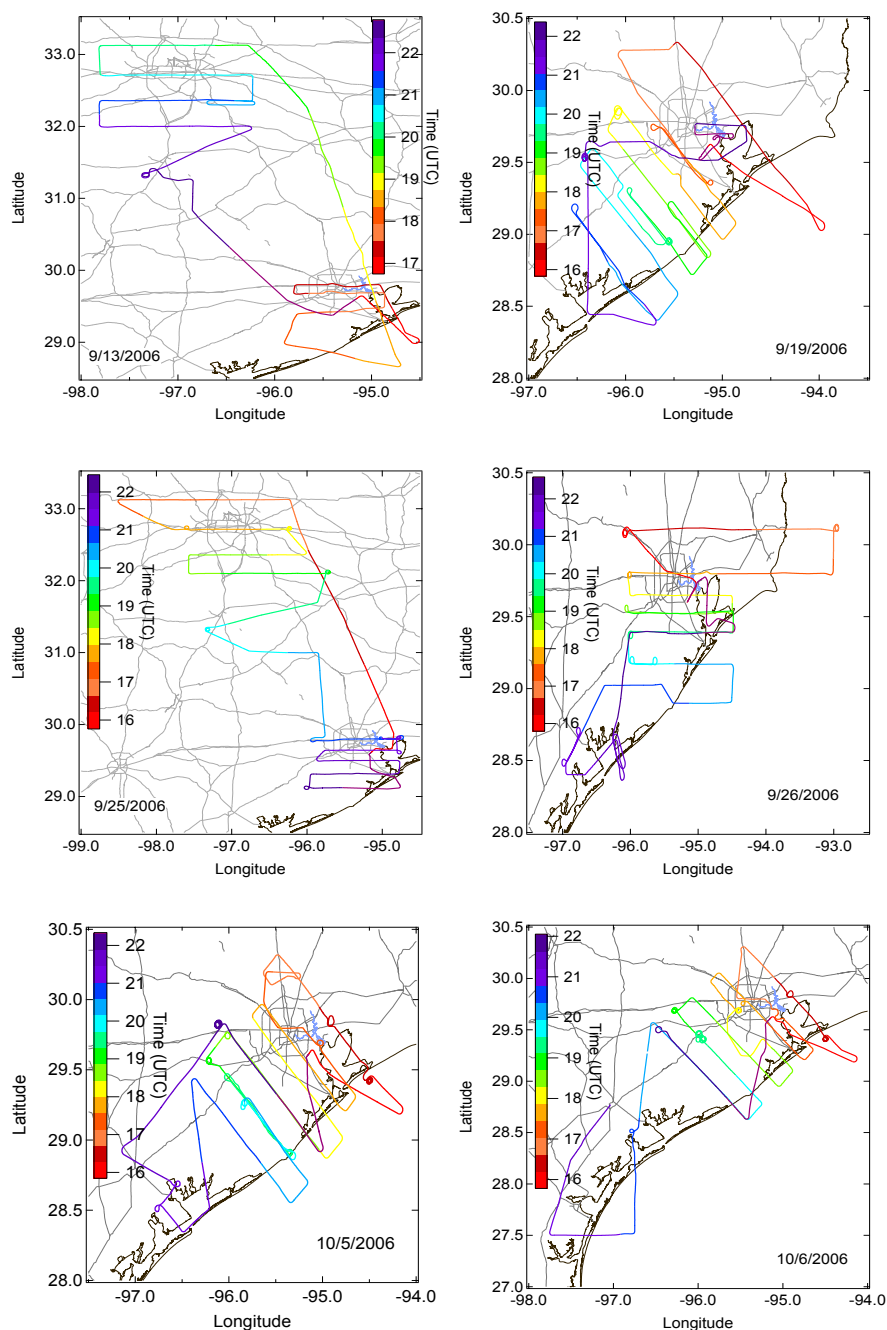


Fig. 2. The flight paths of the NOAA-WP3 aircraft for selected days during TexAQS 2006. Color codes represent the flight times in UTC.

Urban areas are known to have large NO_x emissions because of mobile sources in both the on-road and non-road sectors. According to NEI05-REF, however, the mix of NO_x emission sources in Houston urban area is different from those in other urban areas in Texas. Figure 4 illustrates the contributions of different sectors to the total NO_x emissions in Houston-Galveston in contrast with the Dallas-Fort Worth region. In Dallas-Fort Worth, ~70% of total NO_x emissions is attributed to the mobile sources. In

Houston-Galveston, the mobile sources contribute 39% of total NO_x emissions. Point sources representing a variety of industrial activities and area sources contribute 27% and 34% to total NO_x emissions, respectively. In NEI05-REF, 72% of the NO_x area emissions in Houston-Galveston are from in-port emissions from commercial marine vessels. Within the Houston-Galveston area, the Houston Ship Channel (94.96° W–95.30° W, 29.67° N–29.85° N, as defined in Washenfelder et al., 2010) has an even more unique source

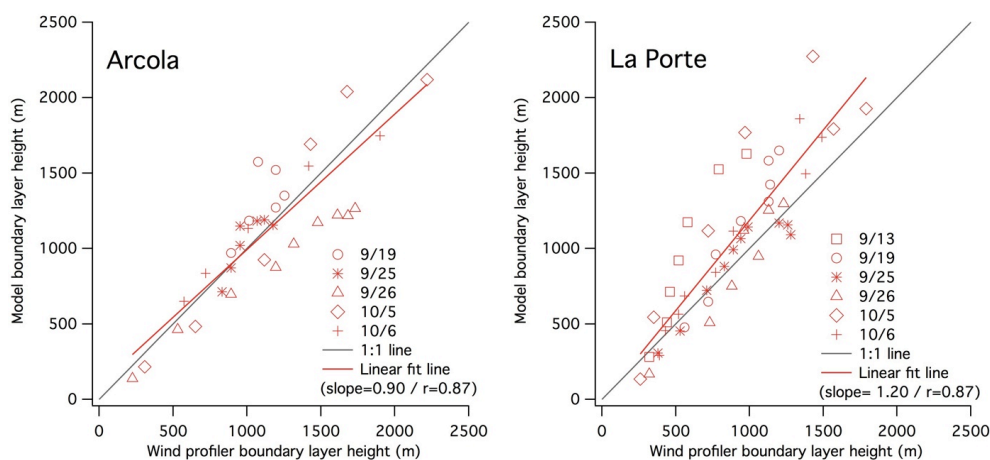


Fig. 3. Comparisons of model atmospheric boundary layer heights with radar wind profiler data at Arcola (29.51° N, 95.48° W) and La Porte (29.67° N, 95.06° W) sites in the Houston-Galveston region. Symbols denote selected dates.

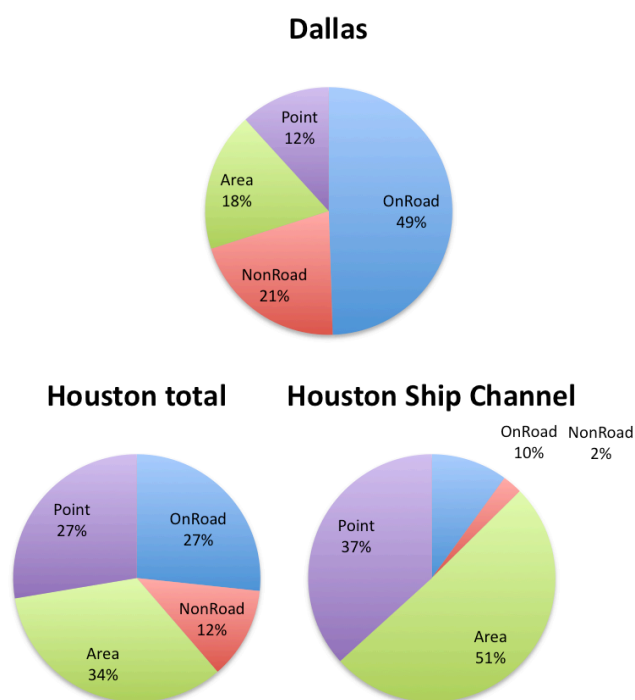


Fig. 4. Partitioning of NO_x emissions in NEI05-REF for Dallas-Fort Worth (see Table 4 for geographic definition), Houston (Table 4), and the Houston Ship Channel area (94.96° W–95.30° W, 29.67° N–29.85° N).

partitioning. Here the mobile source emissions are only 12% of total NO_x emissions. The point and area sources explain 37% and 51% of total emissions, respectively, and 96% of the area source is from in-port emissions from marine vessels. In other words, marine vessel in-port emissions are about 50% of the total NO_x emissions in the Houston Ship Channel box.

Table 4. Geographic information of Texas source boxes used to average satellite and aircraft observations and WRF-Chem model simulations. The dominant source of NO_x emissions in each box is indicated by either C = city or P = power plant.

Name	Center Lon. (°)	Center Lat. (°)	Width Lon. (°)	Width Lat. (°)
C: Dallas-Fort Worth	−96.90	32.95	1.8	1.3
C: Houston-Galveston	−95.30	29.90	1.8	1.4
C: Austin	−97.60	30.50	1.6	1.0
C: San Antonio	−98.40	29.50	1.2	1.0
P: Big Brown & Limestone	−96.30	31.70	1.4	1.0
P: Tolk	−102.55	34.30	1.3	1.0
P: Harrington	−101.65	35.35	1.3	1.1
P: Monticello & Welsh	−94.90	33.25	1.4	1.0
P: Martin Lake	−94.40	32.25	1.4	1.0
P: Mexican power plant	−100.80	28.70	1.4	1.0

4.1.2 Model-simulated and satellite-observed NO₂ columns

In Figs. 5 and 6, the average satellite-retrieved NO₂ columns for the 26 July 2006–6 October 2006 period are compared with model columns for the 10 source boxes defined in Table 4 and shown in Fig. 1. The top panel of Fig. 5 shows SCIAMACHY and model NO₂ columns for each source region, while the bottom panel of Fig. 5 compares the average of 4 OMI NO₂ column retrievals with the model. Because we want to compare the NO₂ columns on a daily basis, we calculate a mean representing each day and then average the daily means for available days. For SCIAMACHY, only 4 days of data are available for Houston and the Mexican power plant. The model biases to SCIAMACHY columns are very consistent for the available days, although the number of sample days is small. Figure 6 focuses on Dallas and

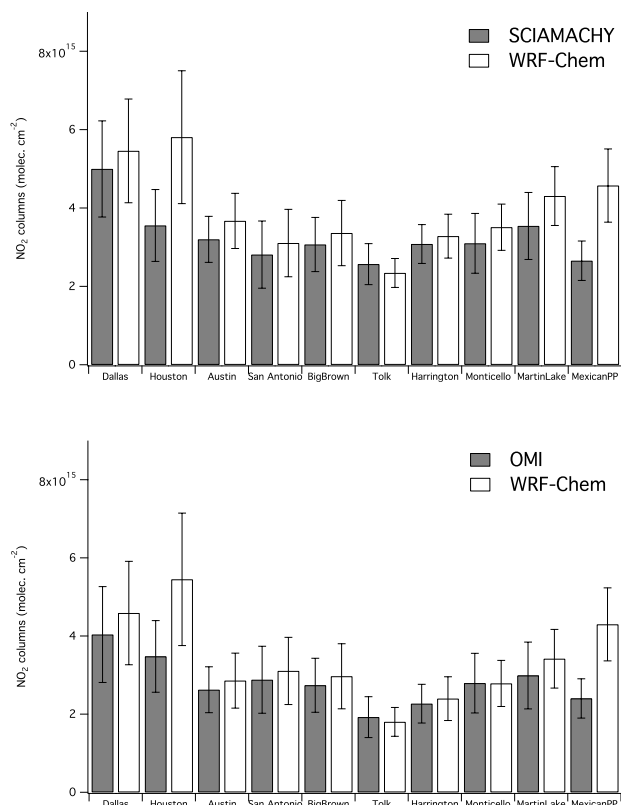


Fig. 5. Comparison of satellite and model tropospheric NO_2 column for various source boxes: (top) U. of Bremen SCIAMACHY and (bottom) averages of 4 OMI retrievals. The four OMI retrievals are produced by KNMI, NASA, and the University of Bremen. Temporal variability (standard deviation) of columns is shown as error bars. The data for 26 July 2006–6 October 2006 are used. For SCIAMACHY (OMI), the numbers of samples are 12(18), 4(14), 11(16), 5(16), 10(16), 9(22), 6(17), 6(21), 14(22), and 4(14) days for Dallas, Houston, Austin, San Antonio, Big Brown and Limestone, Tolk, Harrington, Monticello and Welsh, Martin Lake, and a Mexican power plant, respectively.

Houston only and compares the individual OMI retrievals to the model NO_2 columns.

The model comparisons with SCIAMACHY and the various OMI retrievals are quite similar (Figs. 5 and 6). For most of the regions investigated, with the exceptions of Houston and the Mexican power plant, there is remarkably good agreement between the model NO_2 columns and the satellite retrievals. The consistent agreement of the model NO_2 columns with satellite retrievals from two different instruments and 3 different groups for most Texas cities (except Houston) and for Texas power plants suggests that NO_x emissions for these sources in NEI05-REF are reasonably accurate. Kim et al. (2006, 2009) showed that WRF-Chem model NO_2 simulations that used CEMS data as input reproduced the satellite observations over US power plant sources well. Dallmann and Harley (2010) reported that total mo-

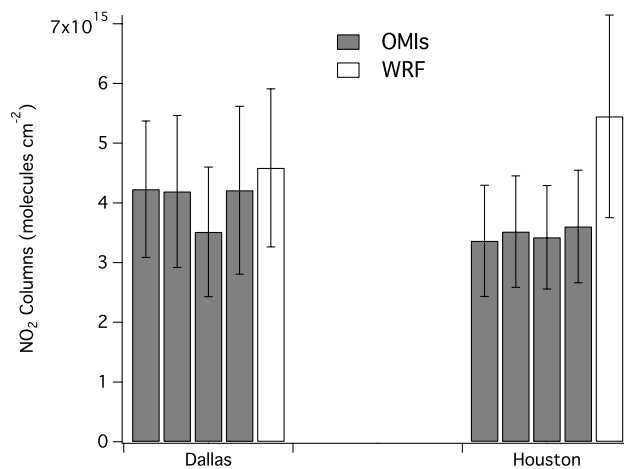


Fig. 6. OMI (U. of Bremen, two KNMI, and NASA products) and model NO_2 columns for the Dallas and Houston boxes. Filled (unfilled) bar represents OMI (WRF-Chem model) columns. Temporal variability (standard deviation) of columns is shown as error bars. The data for 26 July 2006–6 October 2006 are used.

bile source NO_x emissions in NEI-2005 and those estimated by an independent fuel-use-based method were similar, although source contributions to the totals in NEI-2005 and in the fuel-use-based estimation are quite different. That study lends confidence to the NEI-2005 mobile source emissions, and in turn may explain the good agreement between the satellite and the model columns over regions in which mobile sources dominate the total NO_x emissions, which is the case for most cities in Texas (e.g., Dallas, as shown in Fig. 4).

In contrast, the modeled NO_2 columns are more than 50 % larger than the satellite NO_2 columns over Houston and the Mexican power plant region, regardless of which retrieval or instrument is considered (Figs. 5 and 6). The large discrepancy for the Mexican power plant suggests that updates to Mexican point source NO_x emissions in NEI05-REF are required. The Houston region has a unique mix of emissions that includes the mobile sources present in other Texas cities, but also strong industrial and shipping contributions and a major power plant (Fig. 4). As mentioned above, the good model-satellite agreement for other Texas cities, where emissions are dominated by mobile sources, suggests that the mobile source portion of the NEI05-REF is reasonably accurate. We infer that the NEI05-REF should also accurately represent mobile source emissions in Houston. Thus, the discrepancy between the satellite and the model columns in Houston suggests there are uncertainties in Houston's emissions for non-mobile sources. This finding will be explored in more detail in the next section through comparisons of the model with aircraft observations.

4.1.3 Model-simulated and NOAA WP-3D aircraft NO₂

Figure 7 shows a map of the flight path of NOAA WP-3D aircraft together with measured and simulated NO₂ mixing ratios on 13 September 2006, one of two flights from TexAQS 2006 that captured the Dallas-Fort Worth urban plume. Winds were generally northerly on this day, and successive WP-3D transects south of the Dallas area detected the urban plume as it was transported out of the city. The vertical profiles of potential temperature, water vapor mixing ratio, and NO₂ taken to the east of Dallas during the flight show that the model captures the height of the mixed layer well.

The time series of observed and simulated NO₂ for transects downwind of Dallas exhibit excellent agreement (Fig. 7). Table 5 compares the mean WP-3D NO₂ measured during transects within the Dallas-Fort Worth source box defined in Table 4 with the mean model NO₂ using NEI05-REF for both TexAQS 2006 flights in the Dallas area. The 2-flight averages of WP-3D NO₂ and model NO₂ using NEI05-REF in this Dallas box are almost identical (1.68 ppbv and 1.72 ppbv, respectively). In this section, whenever quantitative comparisons between the aircraft data and the model are made, the aircraft observations assigned to the same model grid were averaged so that one-to-one comparison of the two can be made.

Figure 8 shows an analogous example of the WP-3D flight path together with simulated and measured NO₂ over the Houston-Galveston area during the flight on 26 September 2006, when northerly flows predominated across the region. The observed vertical profiles of potential temperature, water vapor mixing ratio, and NO₂ taken just west of Houston during this flight are reproduced well by the simulation, again demonstrating good model performance in terms of meteorology and boundary layer height.

In contrast to the flights over Dallas, NO₂ observations from the 6 daytime flights over Houston deviate substantially from the model predictions. Table 5 summarizes the means of WP-3D NO₂ and the model NO₂ using NEI05-REF for boundary-layer data from these 6 flights within the Houston source box defined in Table 4. Each of the 6 flights shows consistent model overestimates of observed NO₂ over Houston. The model average NO₂ for the 6 flights is 3.32 ppbv, about 60 % above the average WP-3D observed value (2.09 ppbv).

Using the WP-3D observations from each downwind transect, the source region contributing to these model-observed discrepancies over Houston can be isolated. The time series in Fig. 8 demonstrates this approach for the 26 September flight. Upwind of Houston and the Ship Channel, where urban mobile sources should dominate NO_x emissions (transect T1), the simulated NO₂ agrees well with the aircraft observations. However, in transects T2 and T3 downwind of the Houston urban core and Ship Channel, the simulated NO₂ shows substantial deviations from the observations. In particular, in the eastern portions of transects T2 and T3, influ-

Table 5. Mean and standard deviation of WP-3D observed and modeled NO₂ using the NEI05-REF and NEI05-VOCNOX inventories for the Dallas-Fort Worth and Houston-Galveston source boxes. See Table 4 for geographic definition of these source boxes. S.D. = standard deviation.

Date	WP-3D Obs. Mean (S.D.) (ppbv)	NEI05-REF Mean (S.D.) (ppbv)	NEI05- VOCNOX Mean (S.D.) (ppbv)
Dallas			
9/13/2006	1.30 (1.17)	1.47 (1.49)	The same as NEI05-REF
9/25/2006	2.06 (2.64)	1.97 (2.40)	
Average of 2 days	1.68	1.72	
Houston			
9/13/2006	1.53 (2.37)	2.91 (3.90)	1.75 (1.97)
9/19/2006	1.96 (1.91)	2.38 (2.82)	1.73 (1.48)
9/25/2006	1.41 (1.44)	2.74 (3.10)	1.81 (1.82)
9/26/2006	2.83 (3.49)	4.66 (6.58)	2.85 (3.66)
10/5/2006	1.70 (2.25)	3.32 (5.41)	2.38 (3.31)
10/6/2006	3.12 (4.02)	3.90 (4.14)	2.94 (2.65)
Average of 6 days	2.09	3.32	2.24

enced by sources in the Ship Channel, there are large model over-predictions of NO₂. On the western side of these transects, where mobile source emissions from the urban core should dominate, the model is in agreement with the observations.

This behavior, with good model-observation agreement downwind of the Houston urban core and significant disagreements downwind of the Ship Channel, occurred for each of the 6 daytime WP-3D flights focused on the Houston region. In order to quantify these differences, we separated the transect segments downwind of the Houston urban core from the segments downwind of the Ship Channel for each flight. Figure 9 shows how this separation was carried out for the 26 September 2006 flight. The “urban-only” segments of each transect are denoted by black lines on the maps on the left side of Fig. 9. These segments are obtained by examining linear correlations of CO and NO_y (the sum of odd nitrogen species) with CO₂ on each transect. For example, portions of each of the 26 September transects that are over and downwind of the Houston urban core have highly correlated, linear relationships between CO and CO₂ (the black points in the scatter plots on the right side of Fig. 9). These urban-only data correlations have a distinctly larger slope when compared to the transect portions downwind of both Ship Channel itself and the large industrial sources in Mont Belvieu to the north of the Ship Channel (gray points in Fig. 9). A similar separation between the urban-only and mixed urban/industrial portions of each transect is also seen in the NO_y:CO₂ correlations (not shown). Examination of transects from all 6 daytime flights over Houston reveals a

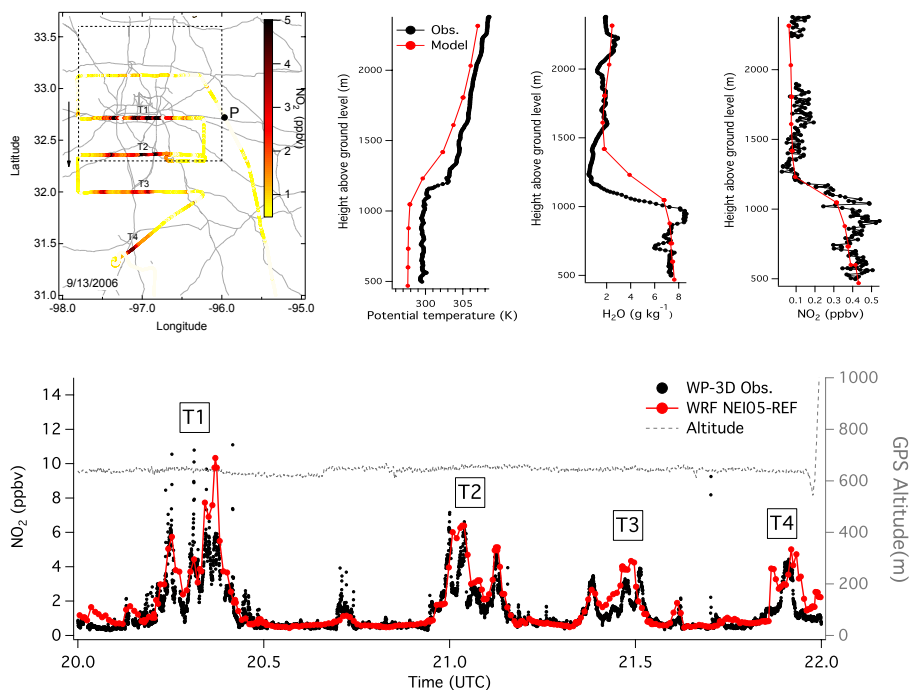


Fig. 7. Map (top left) of the flight tracks on 13 September 2006 capturing Dallas-Fort Worth urban plumes. The WP-3D NO_2 mixing ratio is color-coded over the flight tracks. Arrow denotes a flight track in north-south direction. A box with dashed line on the map is Dallas-Fort Worth region used for the satellite-model comparison (Fig. 1 and Table 4). T1–T4 represent transect 1–4. Vertical profiles of potential temperature, water vapor mixing ratio, and NO_2 measured by the WP-3D at a point “P” on the map are shown (top right). The WRF-Chem model and WP-3D NO_2 for the segments of the flight are compared (bottom).

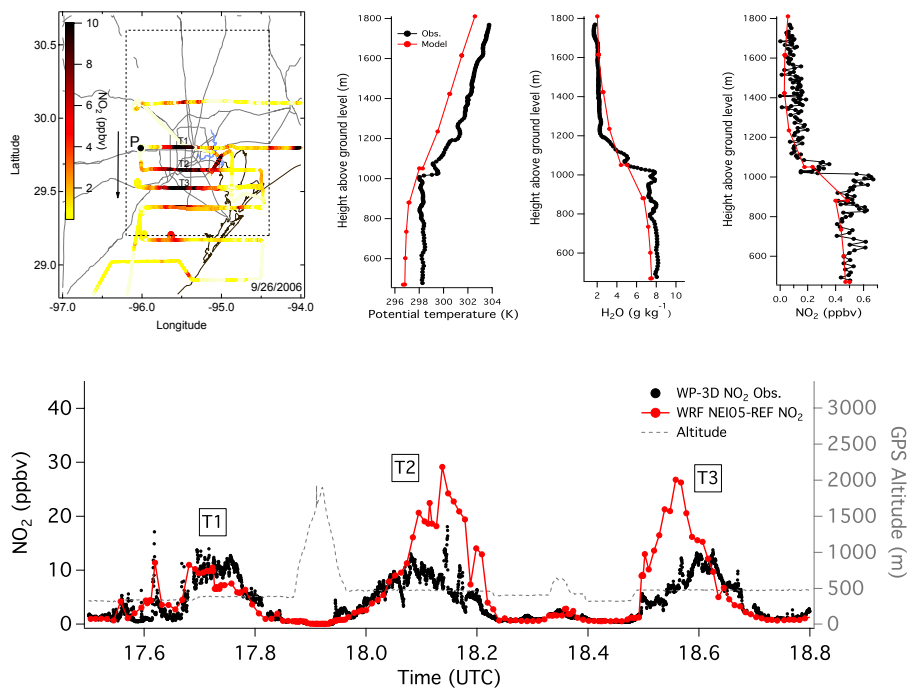


Fig. 8. Map (top left) of the flight tracks on 26 September 2006 capturing Houston urban, industrial, and in-port shipping plumes. The WP-3D NO_2 mixing ratio is color coded over the flight paths. Arrow denotes a flight path in north-south direction. A box with a dashed line on the map is the Houston-Galveston region used for the satellite-model comparison (Fig. 1 and Table 4). T1–T3 represent transects 1–3. Vertical profiles of potential temperature, water vapor mixing ratio, and NO_2 measured at a point “P” on the map are shown (top right). The WRF-Chem model and WP-3D NO_2 for segments of the flight are compared (bottom).

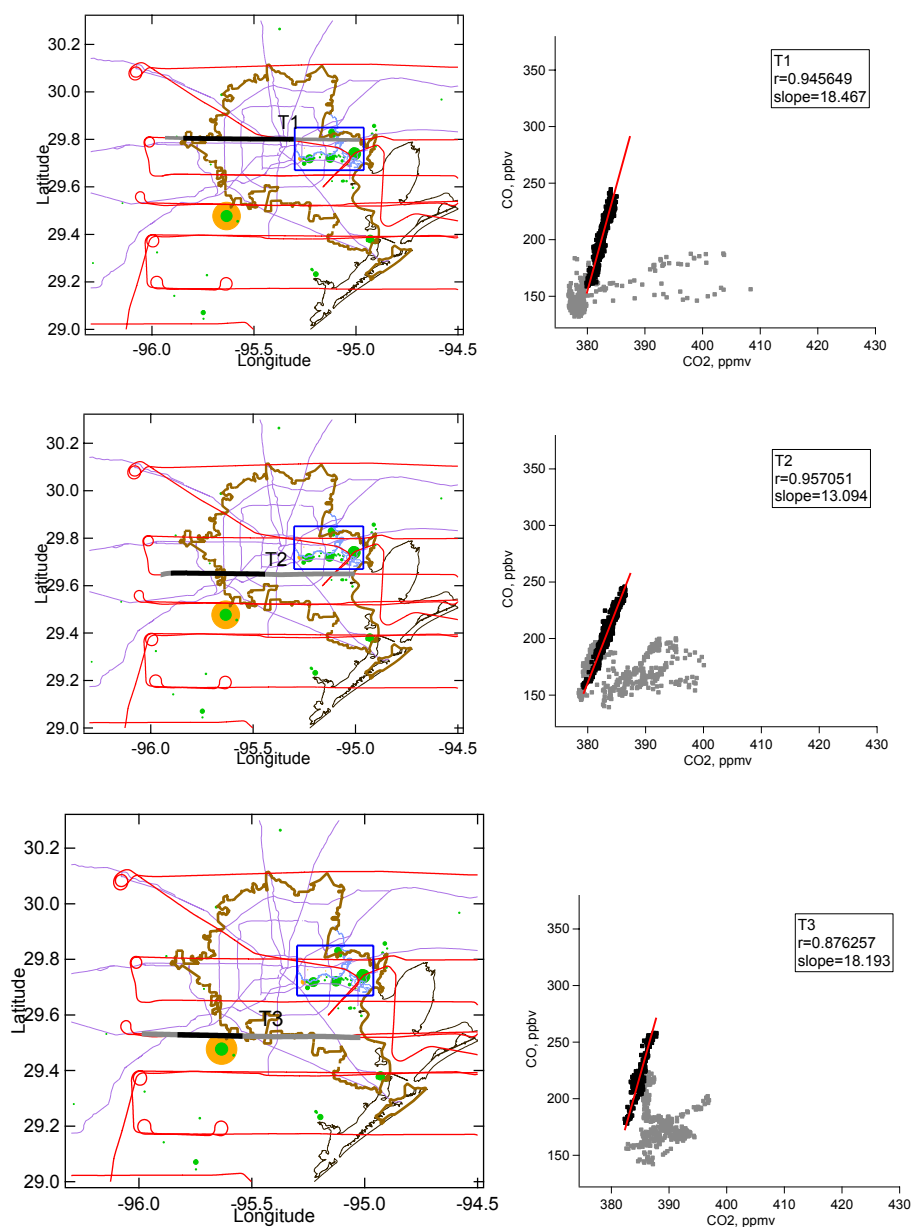


Fig. 9. Flight paths and three transects on the map (left) and scatter plots of CO and CO₂ for each transect (right) on 26 September 2006. Transects T1–T3 (gray colored lines) are the same as in Fig. 8. Black lines (left) and dots (right) in the plots represent the flight segments influenced by urban (mobile) sources. Green (orange) colored circles represent NO_x (SO₂) point sources. Blue box defines the Houston Ship Channel area in this study.

consistent pattern of distinct urban-core-influenced segments on the west side of each Houston transect and Ship-Channel-influenced segments on the eastern portions of the transects.

Figure 10 summarizes the multi-flight averages of the simulated and the WP-3D observed NO₂ for Dallas, Houston, the Houston urban area, and the Houston Ship Channel area. The definitions of the averaging regions used for the Dallas and Houston areas are the same as those for the satellite-model comparisons (Table 4). The “Urban” and “Ship Chan-

nel” averaging areas were defined for each Houston flight using the procedure described in the preceding paragraph. First the daily means for each source box were calculated and the average of the daily means for each source box is plotted (Fig. 10). The picture that emerges from the multi-flight averages (Fig. 10) is consistent with that seen in the individual 13 and 26 September examples (Figs. 7 and 8). The averages of simulated and observed NO₂ are in good agreement over Dallas. For the entire Houston area, model NO₂ is about 60 % higher than the aircraft observations. For the Houston

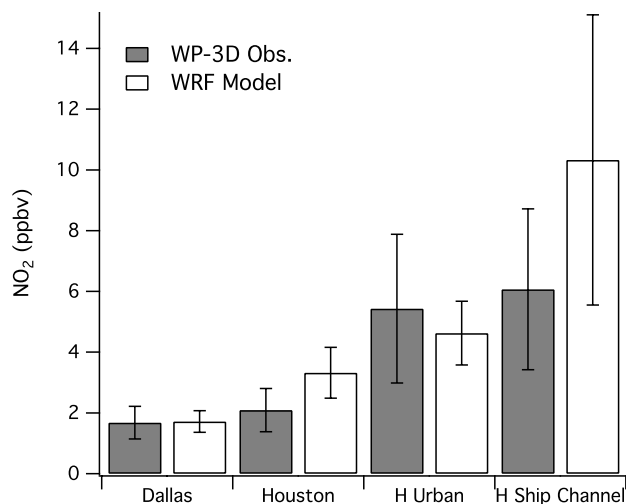


Fig. 10. WP-3D and model NO₂ averaged for Dallas, Houston, Houston urban, and Houston Ship Channel sources. Filled (unfilled) bar represents WP-3D (WRF-Chem model) NO₂. Temporal variability (standard deviation) of columns is shown as error bars. 2 (6) day flight data are used for Dallas (Houston). “Dallas” and “Houston” boxes are the same as the source boxes for satellite-model comparison (Table 4). “H Urban” means the average over the flight segments influenced by urban sources in Houston. “H Ship Channel” denotes the average over the flight segments influenced by industrial and commercial marine vessel sources in the Houston Ship Channel region. Houston Ship Channel flights are defined as in Figs. 9 for 6 daytime flights. The number of samples is 2 (284), 6 (2595), 6 (119), and 6 (142) days (number of the model grids) for Dallas, Houston, Houston Urban area, and Houston Ship Channel area, respectively.

urban-only segments, the model slightly under-predicts the aircraft NO₂ on average. In contrast, the average simulated NO₂ is nearly a factor of 2 higher than the observations for the Ship Channel portions of the Houston flights.

The findings from the model-aircraft NO₂ comparison are consistent with those from the model-satellite NO₂ column comparison. In contrast to good agreement over Dallas-Fort Worth, the model simulations of NO₂ over Houston are about 60 % (50 %–70 %) higher than that of the aircraft (satellite) observations. The aircraft data show that most of the model NO₂ overestimate in the Houston source box appears to be driven by the Ship Channel, whereas NO₂ in the urban core appears to be reasonably well represented by the model. In spite of potential uncertainties in the satellite retrievals, this comparison demonstrates that the large-scale view of NO_x emissions obtained from the satellite data is consistent with the high-resolution picture offered by the aircraft observations, which pinpoint the areas with emission uncertainties. In the next section, we identify the source sectors in the Ship Channel that appear to be the main cause of the NO_x emission discrepancies in the model.

Table 6. NO_x emissions (metric tons as NO₂/day) in NEI05-REF, TCEQ point source emission inventory (EI) in 2006, and DOAS measurements in 2006 (Rivera et al., 2010) for the Houston Ship Channel. The latitude and longitude limits of the Houston Ship Channel used for the NEI05 sums are 29.6700° N–29.8522° N and 94.9619° W–95.3000° W.

Sector	NEI05-REF	TCEQ point source EI or DOAS measurement
Point source	101.0	61.6 * 48.4**
Area source (marine vessel)	139.4 (134.0)	N/A
Onroad source	27.6	N/A
Nonroad source	7.2	N/A
Sum	275.2	82.4***

* TCEQ point source EI used in Washenfelder et al. (2010).

* TCEQ point source EI used in Rivera et al. (2010).

** DOAS measurement in Rivera et al. (2010).

4.1.4 Comparison of NEI-2005 industrial and port NO_x emissions in the Houston Ship Channel area with other inventories and measurements

Biases in tropospheric NO₂ columns and boundary layer NO₂ mixing ratios predicted by the model compared to the satellite and aircraft measurements over the Houston Ship Channel shown in the previous sections suggest that Ship Channel NO_x emissions are too high in the NEI05-REF inventory. As shown in Fig. 4, the two dominant emission sectors in the Houston Ship Channel according to NEI05-REF are the point and area source sectors. In this section, we compare the NEI05-REF inventory values for the Ship Channel with other emission estimates for these activity sectors.

Washenfelder et al. (2010) reported the industrial NO_x emissions in the Houston Ship Channel region based on the Texas Commission on Environmental Quality (TCEQ) point source emission inventory compiled specifically for the Texas AQS 2006 time period. The Ship Channel point sources in NEI05-REF emit a total of 101 tonnes day⁻¹, which is ~64 % higher than the TCEQ 2006 point source inventory for roughly the same region (Table 6). The Ship Channel’s point sources are a complex mix of facilities that are involved in some way with the petrochemical industry, along with a smaller number of electrical power plants and electricity co-generation facilities. The emissions for the power/co-generation plants were updated to August 2006 levels using the CEMS database. However, a major fraction (~69 %) of the NEI05-REF point emissions within the Houston Ship Channel source box are from facilities not reporting in the CEMS database. The emissions of these facilities are instead applicable to 2002, since they were not updated from their NEI-2002 levels in the NEI-2005 version used here. Thus, part of the model-observed NO_x discrepancy in the Ship Channel may be due to mandated NO_x emission reductions

Table 7. Annually averaged port emissions (tonnes yr⁻¹) for SO₂, NO_x, VOC, CO, and PM_{2.5} for Harris County from the NEI-2005 inventory, and for the Port of Houston from US EPA (2007). The emission mass ratios of NO_x to SO₂ are also given.

NEI-2005 SCC or Data Source	SCC Description or Representative Area	SO ₂	NO _x	VOC	CO	PM _{2.5}	NO _x /SO ₂
2280002100	CMV, diesel, port	1790	39516	1235	5210	1529	22.08
2280003100	CMV, residual, port	5548	10543	329	1387	423	1.90
2280002200	CMV, diesel, underway	9	195	6	26	8	21.67
2280003200	CMV, residual, underway	40	54	2	1	3	1.35
NEI-2005 (Sum of CMV)	Harris County total	7387	50308	1572	6624	1962	6.81
EPA Report (2007)	Port of Houston	4136	4597	158	346	491	1.11

between 2002 and 2006 for point sources that are not reflected in NEI05-REF.

The NO_x area source sector for the Houston Ship Channel within NEI-2005 is dominated (134.0 tonnes day⁻¹ = 96 %) by port emissions from commercial marine vessels (CMVs) (Table 6). The US EPA (2007) report on Commercial Marine Port Inventory Development 2002 and 2005 gives a highly detailed accounting of CMV emissions for the Port of Houston applicable to 2002, which differs markedly from the NEI-2005 emissions, in particular for NO_x. Table 7 compares annual averages of 5 species for the Port of Houston from the EPA report and the emissions of these species from CMV activity in Harris County from NEI-2005; the Port of Houston lies completely within Harris County and is the primary area of CMV activity there. While the Harris County SO₂ emissions from NEI-2005 are only 80 % higher than the US EPA (2007) Port of Houston emissions, the NEI-2005 NO_x emissions are a factor of 11 higher than US EPA (2007), with CO and VOC showing similar order-of-magnitude differences between NEI-2005 and US EPA (2007). Also shown in Table 7 are the sums for the 4 Source Classification Codes (SCC) classes contributing to Harris County CMV emissions within NEI-2005. Emissions from diesel fuel sources predominate over residual fuel sources for all species except SO₂. Details on the emission factors, activity rates, and other important parameters are not available within the NEI-2002/2005 inventory description (US EPA, 2008). In contrast, residual fuel sources account for nearly all port activity emissions within the more comprehensive US EPA (2007) report.

Based on the data in Table 7, NO_x to SO₂ emission ratios are a factor of six higher for NEI-2005 than in the US EPA (2007) report. Furthermore, NO_x/SO₂ emission factor ratios from US EPA (2007) are more than a factor of 10 lower for CMVs using diesel fuel than the diesel fuel emission ratios from NEI-2005 in Table 7. NO_x/SO₂ emission factor ratios for CMVs using residual fuel within US EPA (2007) are also a factor of 2 (or more) lower for most ship classes than those in NEI-2005. NO_x/SO₂ emission ratios determined from ship plume sampling during TexAQS-2006 (Williams et al., 2009) are more consistent with the US EPA (2007) re-

port than with the NEI-2005 port emissions. Though only a few plumes close to port were actually sampled by Williams et al. (2009), emission ratios were similar to the many plumes sampled from similar ships anchored in the Gulf of Mexico. Mean NO_x/SO₂ mass emission ratios from these ships range from 0.58 for crude oil tankers to 2.19 for bulk freight carriers.

It is important to note that port emissions within NEI05-REF are identical to those in the most recent NEI-2005 version 4.1 inventory, released 23 March 2011 (SMOKE-ready emission file ar-inv_lm_no_c3_cap2002v3_20feb2009_v0_orl.txt). For other US ports within NEI-2005, the NO_x/SO₂ emission factor ratios for CMVs using diesel fuel are similar to those for Harris County (within a factor of 2). Thus, all users of NEI-2005 should be aware of the significant overestimate of NO_x port emissions throughout the US.

Rivera et al. (2010) estimated the total NO_x emissions from the Houston Ship Channel area (29.65° N–29.80° N, 94.98° W–95.28° W, a slightly different definition of the Ship Channel than ours) using a mini-differential optical absorption spectroscopy (DOAS) instrument during TexAQS 2006. Their estimation of the total Houston Ship Channel NO_x emissions is 82.4 tonnes day⁻¹ (75.5–89.4 tonnes day⁻¹ using mean absolute deviation from the median). Rivera et al. (2010), using a different version of the TCEQ 2006 point source emission inventory than that used in this work, calculated Ship Channel point source emissions of 48.4 tonnes day⁻¹ (Table 6). Thus, according to Rivera et al. (2010)'s estimation, the NO_x emissions from non-point sources in the Houston Ship Channel are 34.1 tonnes day⁻¹ (27.0–41.0 tonnes day⁻¹). The NEI-2005 NO_x emissions from non-point sources are 174.2 tonnes day⁻¹, ~5 times as large as that in Rivera et al. (2010). The total NO_x emissions (82.4 tonnes day⁻¹) reported by Rivera et al. (2010) are about 30 % of those (275.2 tonnes day⁻¹) in the NEI-2005. This finding is consistent with the fact that our model NO₂ simulations in Houston are much higher than those in satellite and aircraft observations.

These comparisons of the NEI-2005 with other emission inventories and with estimates based on measurements in the

Houston Ship Channel indicate that the industrial NO_x emissions in the NEI-2005 may be too high by about 60% and that the largest uncertainties in the NEI-2005 NO_x emissions in this area may come from in-port ship emissions in the region.

4.2 Modification of NEI-2005 VOC and NO_x emissions

4.2.1 Increases of NEI-2005 propylene and ethylene emissions using Solar Occultation Flux measurements

Direct and indirect evidence of inventory underestimates of ethylene (C₂H₄) and propylene (C₃H₆) emissions from the petrochemical facilities in the Houston area has previously been documented. For example, Wert et al. (2003) showed that C₂H₄ and C₃H₆ emissions from two major refineries near Freeport and Sweeny were underestimated by a factor of 50 to 100 when compared to emissions derived from Electra aircraft observations from TexAQS 2000. These underestimates were additionally shown to be responsible for serious HCHO and O₃ under-predictions in a simple plume dispersion model (Wert et al., 2003). Likewise, Jiang and Fast (2004) and Byun et al. (2007) showed much better agreement between model and observed O₃ levels in the Houston region when C₂H₄ and C₃H₆ emissions in the Ship Channel area were increased by factors of 6 to 8.

The Solar Occultation Flux (SOF) measurements of C₂H₄ and C₃H₆ emissions reported in Mellqvist et al. (2010) allowed direct comparisons with the NEI05-REF inventory for 14 different point source locations in southeast Texas during the TexAQS 2006 campaign. Ten of these locations are within the Houston Ship Channel or directly east of Houston, while the other 4 sites are major petrochemical facilities to the south and southeast of Houston. As shown in Fig. 11 (blue circles), the standard NEI05-REF inventory significantly under-predicts the observed SOF emissions for both C₂H₄ and C₃H₆.

A modified inventory, NEI05-VOC, was generated to assess the impact of the low C₂H₄ and C₃H₆ emissions in NEI05-REF on the WRF-Chem simulations. In contrast to across-the-board VOC emission increases over the Ship Channel used in previous studies (e.g., Jiang and Fast, 2004; Byun et al., 2007), the NEI05-VOC included adjustments of activity-specific emission factors related to the petrochemical facilities sampled by the SOF measurements. These modifications used the information within the US EPA's SCCs for the major C₂H₄ and C₃H₆ point sources and for each of the 14 locations sampled by Mellqvist et al. (2010). Because of ambiguity in how facilities report activity-specific VOC emissions, and to keep the analysis of the emissions from dozens of SCCs tractable, eight broad categories were constructed from analysis of the major SCCs contributing to C₂H₄ and C₃H₆ emissions within NEI05-REF. These eight categories are listed in Table 8, along with the SCCs assigned

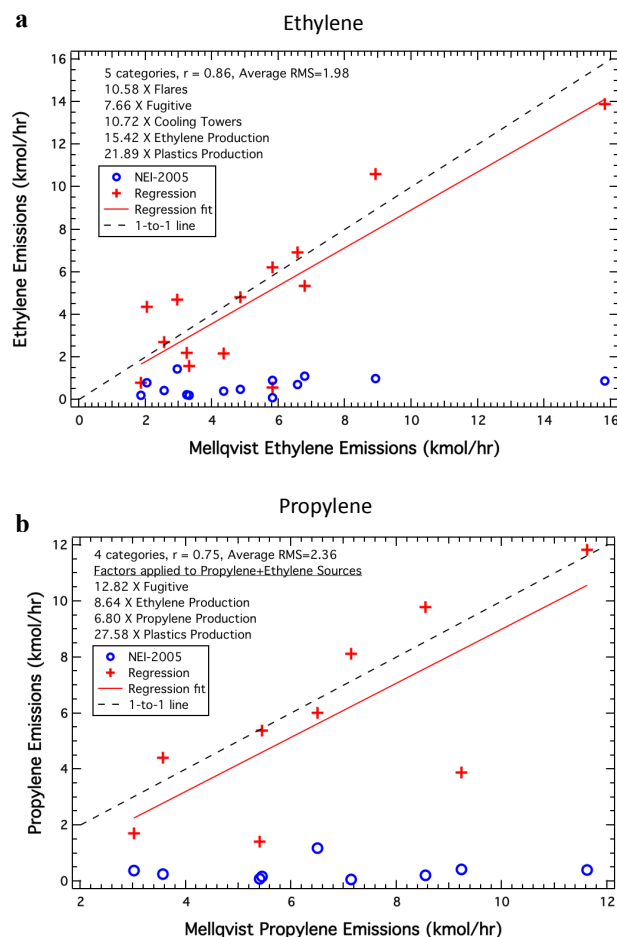


Fig. 11. Updated and default ethylene and propylene emissions in NEI-2005 in comparison with emission estimates by Mellqvist et al. (2010).

to each category. Many other SCCs with relatively minor emissions are lumped into an “Other” category.

For either C₂H₄ or C₃H₆, multiplication factors (M_i , $i = 1, 8$) for the emission categories are then numerically determined to yield a best fit to the linear system:

$$[A_{i,j}] \cdot M_i \approx \text{OBS}_j - \text{Other}_j \quad (1)$$

where $[A_{i,j}]$ is the matrix of NEI05-REF emissions for source category i and location j , and OBS_j are the average SOF observations at location j . Table 9 gives the elements of $[A_{i,j}]$ and Other_j from NEI05-REF for ethylene. The M_i vector for the over-determined system is solved by linear least squares using QR/LQ matrix decomposition from the LAPACK library (SIAM, 1999). In practice some of the M_i solution values are negative, yielding a multiplication factor with a non-physical meaning. If a negative M_i is calculated, the NEI05-REF emissions from that category are added to the “Other” vector, the number of source categories is reduced by one, and the M_i vector in Eq. (1) is solved again.

Table 8. Eight emission categories used in ethylene and propylene NEI-2005 emission perturbations, their 8-digit US EPA Source Classification Codes, and brief descriptions of each.

Flares	
30600999	Petroleum Industry, Flares, Not Classified
30600904	Petroleum Industry, Flares, Process Gas
39990024	Miscellaneous Manufacturing Industries, Process Gas, Flares
39990022	Miscellaneous Manufacturing Industries, Residual Oil, Flares
Fugitives	
30188801	Chemical Manufacturing, Fugitive Emissions, General
30180001	Chemical Manufacturing, General Processes, Fugitive Leaks
30688801	Petroleum Industry, Fugitive Emissions, General
30600819	Petroleum Industry, Fugitive Emissions, Compressor Seals, Gas Streams
30600820	Petroleum Industry, Fugitive Emissions, Compressor Seals, Heavy Liquids
Cooling Towers	
38500101	Cooling Tower, Process Cooling, Mechanical Draft
38500102	Cooling Tower, Process Cooling, Natural Draft
30600701	Petroleum Industry, Cooling Towers
Miscellaneous	
30199998, 30199999	Chemical Manufacturing, Other Not Classified, General
30119799	Chemical Manufacturing, Olefin Production, Not Classified
30699998, 30699999	Petroleum Industry, Unclassified Petroleum Products, Not Classified
Storage/Transfer	
30183001	Chemical Manufacturing, General Processes, Storage/Transfer
Ethylene Production	
30101812	Chemical Manufacturing, Plastics Production, Polyethylene – Low Density
30101807	Chemical Manufacturing, Plastics Production, Polyethylene – High Density
30117401	Chemical Manufacturing, Plastics Production, Ethylene Oxide, General
30119701	Chemical Manufacturing, Plastics Production, Olefin Production, Ethylene – General
Propylene Production	
30119705	Chemical Manufacturing, Olefin Production, Propylene – General
30119709	Chemical Manufacturing, Olefin Production, Propylene – Fugitives
30101802	Chemical Manufacturing, Olefin Production, Plastics Production, Polypropylene and Copolymers
Plastics Production	
30101809	Chemical Manufacturing, Plastics Production, Extruder
30101813	Chemical Manufacturing, Plastics Production, Recovery and Purification
30101816	Chemical Manufacturing, Plastics Production, Transfer-Handling-Loading
30101899	Chemical Manufacturing, Plastics Production, Other not specified
30101811	Chemical Manufacturing, Plastics Production, Storage
30101810	Chemical Manufacturing, Plastics Production, Conveying

Some remaining positive M_i factors make a negligible contribution to the overall goodness of the fit to the observed emissions. In that case, the r-coefficient and RMSE values are calculated with each remaining M_i factor to further eliminate unnecessary factors. The resulting 5 best-fit multiplication factors for ethylene are given in Fig. 11a, along with the linear fit to observations. The NEI05-VOC point source

ethylene emissions are calculated by multiplying the SCC-specific C₂H₄ emissions (Table 9) in NEI05-REF by the factors listed in Fig. 11a.

For propylene, only nine locations have reported C₃H₆ fluxes, and the same least-squares approach results in poor comparisons with the average SOF observations when the categories with negative M_i factors are removed from

Table 9. Diurnally averaged ethylene emissions (mole h⁻¹) from the NEI-2005 inventory for the 14 locations with ethylene emissions reported in Mellqvist et al. (2010) and for the eight emission categories given in Table 8. “HSC” refers to the 7 Mellqvist et al. (2010) sectors within the Houston Ship Channel. “Other” refers to additional emissions at each location not within the eight emission categories.

Facility Location	Flares	Fugitive	Cooling Towers	Misc.	Storage/Trans.	C ₂ H ₄ Prod.	C ₃ H ₆ Prod.	Plastics Prod.	Other
HSC-1	128.3	15.4	2.8	4.3	0.1	0.	0.	0.	53.9
HSC-2	5.4	255.1	3.0	36.6	44.8	0.	0.	0.	50.0
HSC-3	0.	597.5	27.6	335.2	66.2	0.	0.5	0.	60.4
HSC-4	0.	136.9	17.0	12.9	5.3	0.	0.1	42.2	20.1
HSC-5	0.	79.3	5.1	18.4	7.0	356.3	0.	23.9	213.7
HSC-6	0.	74.4	0.5	36.7	5.9	0.	0.	4.8	71.3
HSC-7	0.	161.1	112.2	44.3	0.	0.	0.1	6.1	93.3
Bayport	0.	369.4	10.6	121.	7.2	175.3	2.8	10.6	203.3
Channelview	0.	522.7	11.0	207.5	3.4	0.	0.	0.	29.0
Chocolate Bayou	0.	143.6	7.2	49.4	0.	228.3	0.	1.3	41.7
Freeport	16.7	96.1	22.4	38.4	27.7	589.2	0.	4.8	177.1
Mount Belvieu	9.0	8.6	14.6	2.2	0.5	635.9	16.6	170.7	9.9
Sweeny	0.	35.5	25.6	0.6	0.1	0.	0.6	0.	10.3
Texas City	131.0	175.0	85.0	144.8	895.4	0.	0.	0.	9.5

Eq. (1). But as shown in Fig. 11b, when the sum of the C₂H₄ and C₃H₆ emissions are used as elements of $[A_{i,j}]$, a good correlation with the average SOF observations is obtained with 4 multiplication factors. The NEI05-VOC point source propylene emissions are therefore calculated by multiplying the SCC-specific C₂H₄ plus C₃H₆ emissions (Table 9) by the factors listed in Fig. 11b.

The above fitting procedure updated ethylene and propylene emissions by comparison of the NEI-2005 with the average SOF observations at each of the point source locations studied by Mellqvist et al. (2010). The emission estimates derived from SOF have an estimated uncertainty of 35 % due to the measured variability in the wind direction between the source and the sampling point and also from assumptions of rapid vertical mixing. Moreover, when sampling in the same locations multiple times during the TexAQS 2006 study period, Mellqvist et al. (2010) noted variations in the SOF-derived estimates of ethylene and propylene emissions; depending on the source region, their estimates varied between sampling periods by as much as 60 % for ethylene and 90 % for propylene. The updated ethylene and propylene emissions in NEI05-VOC do not account for either of these effects; instead, these updates should be thought of as representing only typical emission conditions encountered during TexAQS 2006. However, uncertainty and variability in ethylene and propylene emission fluxes must be considered when applying this updated inventory to modeling specific flights, as is discussed further in Sect. 4.3.

4.2.2 Reductions of NEI-2005 NO_x emissions in the Houston Ship Channel

In Sect. 4.1, NEI05-REF NO_x emissions in the Houston Ship Channel were shown to be too high. For example, NEI05-REF NO_x emissions in the Houston Ship Channel are about 3 times higher than those measured by Rivera et al. (2010) in 2006. The potential causes for this discrepancy appear to be overestimates of industrial and port ship emissions. In order to understand the impact of these NO_x overestimates on WRF-Chem ozone and highly reactive VOC predictions, we generated another modified version of the NEI-2005, NEI05-VOCNOX. Starting from the NEI05-VOC discussed in Sect. 4.2.1, we made two changes: we decreased the industrial NO_x emissions by 50 %, and we eliminated the port ship emissions. These modifications result in a reduction of the total NEI05-REF NO_x emissions across the Houston Ship Channel of 70 %. In the NEI05-VOCNOX, total NO_x emissions in the Houston Ship Channel are ~85 tonnes day⁻¹, similar to the measurements by Rivera et al. (2010).

Brioude et al. (2011) used a top-down inversion method to derive an a posteriori emission inventory for the Houston-Galveston area, using NEI05-REF as a priori. This independent approach draws a similar conclusion as the current study: NO_x emissions are overestimated in the Houston Ship Channel by about a factor of 2.

4.3 Comparisons of aircraft observations with model simulations using the NEI-2005 reference and updated emission inventories

Figure 12 shows the time series of WRF-Chem model results with the three emission inventories (NEI05-REF, NEI05-VOC, NEI05-VOCNOX) compared to WP-3D observations of NO₂, ethylene, propylene, formaldehyde, and O₃ for the Houston portion of the 26 September 2006 flight shown in Fig. 8. The detailed comparisons for NO₂, for ethylene and propylene, and for HCHO and O₃ are discussed separately in the following sections.

4.3.1 NO₂

The NO₂ simulations with NEI05-VOCNOX show remarkably good agreement with the observations, whereas the simulated NO₂ with either NEI05-REF or NEI05-VOC shows the discrepancy with the observations as discussed above. Table 5 summarizes, for the Houston-Galveston source box defined in Table 4, the mean NO₂ observed by the WP-3D in the boundary layer from all 6 TexAQS 2006 daytime flights along with the mean model NO₂ for the same locations using the NEI05-REF and the NEI05-VOCNOX inventories. Because the NO₂ simulations from the NEI05-REF and the NEI05-VOC are almost identical, the results from the NEI05-VOC are omitted in Table 5. The mean of the model NO₂ using NEI05-VOCNOX for the 6 daytime flights is 2.24 ppbv, which is ~50 % lower than that of NEI05-REF and ~10 % higher than that of the average WP-3D observations.

4.3.2 Ethylene and propylene

As expected, the modeled ethylene and propylene mixing ratios with NEI05-VOC and NEI05-VOCNOX are much larger than those simulated with NEI05-REF (Figs. 12 and 13, Table 10). The reduction of Houston Ship Channel NO_x using the NEI05-VOCNOX inventory decreases the modeled ethylene and propylene mixing ratios compared to using NEI05-VOC, because lower NO₂ levels lead to increased hydroxyl radical (OH) mixing ratios that consequently result in a faster sink for these alkenes.

In TexAQS 2006, the WP-3D had two methods for measuring ethylene: canisters analyzed post-flight by the whole air sampler (WAS) system (Schauffler et al., 1999, 2003) and the continuous measurements by the laser photo-acoustic spectroscopy (LPAS) instrument (de Gouw et al., 2009). The LPAS ethylene measurements were made with much higher frequency than the WAS canisters were sampled, and LPAS data were available on more flights than WAS. On the other hand, the WAS analyzer had higher precision and better sensitivity to ethylene than the LPAS instrument.

On the 26 September flight (Fig. 12), the simulated ethylene with NEI05-VOC or NEI05-VOCNOX sometimes agrees better with the ethylene measurements by WAS and

LPAS. There are also occasions in which the model results do not capture the observed peaks of the ethylene plumes, as well as times when the model peaks are much larger than the observed ones. The latter situation is discussed further below. An example of the former situation can be seen in the observed ethylene plumes at 07:15–17:30 UTC, 18:15–18:30 UTC and 19:00–19:15 UTC, which can be traced back to the Beaumont/Port Arthur area. While the updates to the ethylene emissions in NEI05-VOC/NEI05-VOCNOX were applied to all processes listed in Table 8 wherever they occurred in the model domain, SOF observations were not made in Beaumont/Port Arthur. It is possible that the ethylene emission adjustment factors derived from the SOF observations in and around Houston are not generally applicable to ethylene emissions from petrochemical facilities in other areas. Another possibility is that there are additional processes besides those in Table 8 that lead to high ethylene emissions in Beaumont/Port Arthur, in which case the inventory adjustment procedure discussed in Sect. 4.2.1 would not increase ethylene emissions sufficiently in that region.

Figure 13 compares flight averages of the model and the ethylene measurements for the WP-3D flight legs within the boundary layer and the Houston-Galveston source box (defined in Table 4). The model results in Fig. 13 were sampled only at the times and locations in which the measurements were made before calculating averages.

For the WAS measurements of ethylene, the model results with the default emission inventory (NEI05-REF) are consistently 50%–70 % lower than the observations (Fig. 13). The simulations with NEI05-VOC and the NEI05-VOCNOX agree with the WAS observations within –20 % to +30 %, except for 26 September when the model ethylene with NEI05-VOCNOX (NEI05-VOC) is ~50 % (65 %) higher than the observations. The overall Houston-area boundary layer averages from the 5 flights where WAS data were available (Table 10) similarly show much better agreement between the WAS ethylene and the model simulations using either NEI05-VOC or NEI05-VOCNOX, with NEI05-VOCNOX providing the smallest overall model-measurement discrepancy.

For the LPAS measurements of ethylene, the model runs with NEI05-REF are consistently low by 35%–64 %, similar to the model-WAS comparison (Fig. 13). The simulated ethylene mixing ratios using either NEI05-VOC or NEI05-VOCNOX are persistently higher than the LPAS measurements by 17%–51 % for most of the days (64%–78 % above the observation on 26 September). Averages from the 6 Houston flights where boundary-layer LPAS measurements of ethylene were available (Table 10) show that the model results with NEI05-VOCNOX (NEI05-VOC) are 38 % (43 %) larger than the LPAS observations. Despite larger model-observed discrepancies with the LPAS data than with the WAS observations, NEI05-VOCNOX is overall the best of the three inventories used in the model simulations of ethylene, as was the case for the WAS data.

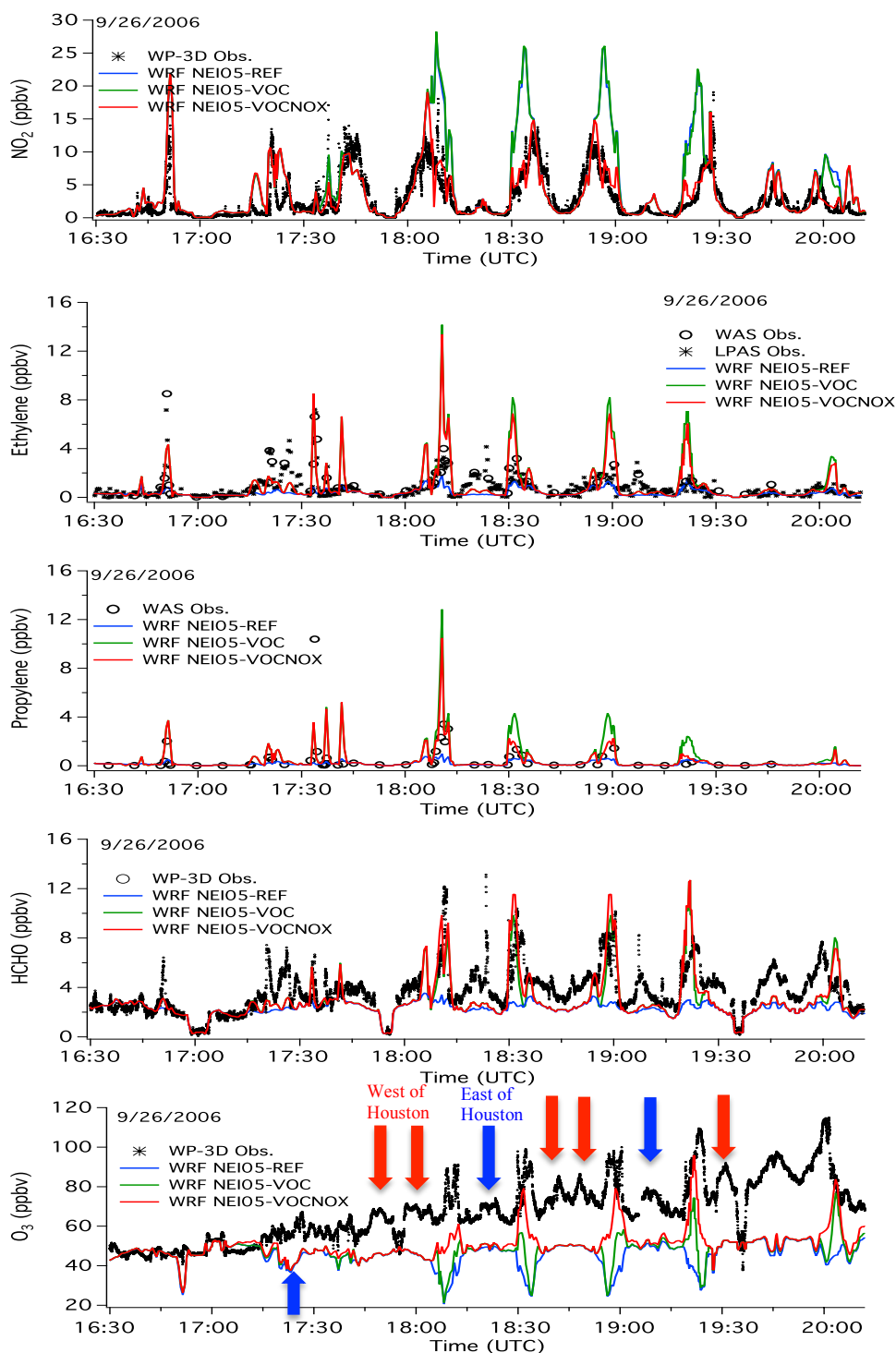


Fig. 12. WP-3D observed and simulated NO₂, ethylene, propylene, formaldehyde, and O₃ on 26 September, 2006. The red and the blue arrows denote the west and the east of Houston, respectively.

The model simulations with NEI05-VOC and NEI05-VOCNOX show enhanced propylene at the times when the measurements detected the plumes on 26 September (Fig. 12), while the model with NEI05-REF cannot produce

elevated mixing ratios of propylene. For all boundary layer Houston flight legs investigated, the model propylene with NEI05-REF is consistently lower by 60%–90% than the whole air sampler measurement, except for 19 September

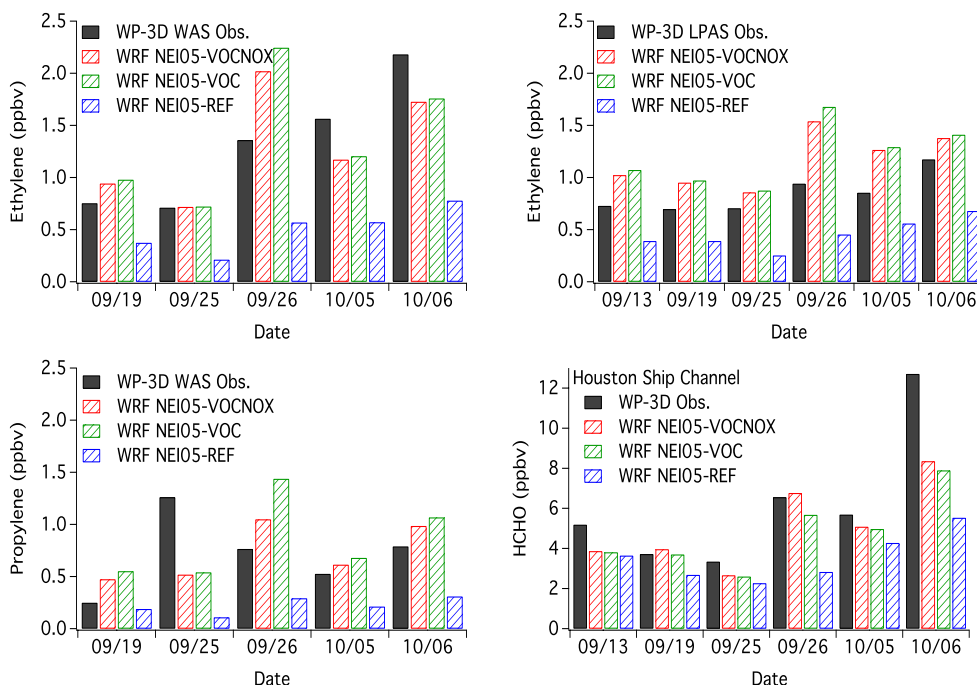


Fig. 13. Plots comparing observed ethylene, propylene, and formaldehyde (<1 km altitude above ground level) with the model results using the NEI05-REF, NEI05-VOC, and NEI05-VOCNOX inventories over the Houston area. For formaldehyde, the data over the Houston Ship Channel area are used.

Table 10. Averages of observed and modeled ethylene and propylene for the model simulations using NEI05-REF and NEI05-VOC. WAS denotes the whole air sampler and LPAS stands for the photoacoustic measurement of ethylene.

VOC	WP-3D Obs. (ppbv)	WRF NEI05- REF (ppbv)	WRF NEI05- VOC (ppbv)	WRF NEI05- VOCNOX (ppbv)
WAS Ethylene	1.31	0.50	1.38	1.32
LPAS Ethylene	0.85	0.45	1.22	1.17
WAS Propylene	0.72	0.22	0.86	0.73
Formaldehyde	4.12	3.2	3.77	3.78
Formaldehyde (Ship Channel)	6.20	3.54	4.78	5.12

in which the model with NEI05-REF and the observations agree better than the simulations with the other inventories (Fig. 13). On 26 September, the simulated propylene mixing ratios with NEI05-VOC are higher than the measurements, but the simulations with NEI05-VOCNOX agree better with the measurements (Fig. 12). The model-simulated propylene with NEI05-VOC is 30%–120% higher than the whole air sampler propylene observations except for 25 September (Fig. 13). The simulations with NEI05-VOCNOX reduce the biases in the model propylene on most days, such that the simulated propylene is 20%–90% higher than the observa-

tions (except for 25 September). For the 5 flight days with boundary layer WAS data in the Houston source box (Table 10), the overall average propylene mixing ratios from the model with NEI05-VOCNOX (0.73 ppbv) and the whole air sampler (0.72 ppbv) are nearly identical.

In summary, the ethylene and propylene mixing ratios modeled with the updated inventories based on the 2006 SOF observations downwind of petrochemical facilities emissions (i.e., NEI05-VOC or NEI05-VOCNOX) compare better with the WP-3D observations than simulated mixing ratios using the reference NEI-2005 inventory. On any particular day, the use of the average SOF observations to adjust the ethylene and propylene emissions does not give precise agreement between modeled and aircraft-observed mixing ratios. This behavior highlights the variability in the ethylene and propylene emissions from petrochemical facilities around Houston, a phenomenon noted by other investigators (Murphy and Allen, 2005; Mellqvist et al., 2010). In particular, Mellqvist et al. (2010) documented variations in SOF-measured ethylene and propylene emissions of as much as 60% and 90%, respectively, when sampling the same Ship Channel source regions multiple times in the same day or on different days during TexAQS 2006. The use of average ethylene and propylene emission rates to adjust the petrochemical facility emissions in the model inventory is obviously a simplification, but without detailed information on the variability of the many ethylene/propylene point sources in the region on

each flight day, one cannot expect a perfect simulation on any given day. Nevertheless, the flight-to-flight discrepancies between the observations and the model with the updated emissions are well within the known variability of the Ship Channel's ethylene and propylene sources.

4.3.3 Formaldehyde and O₃

The high time resolution tunable diode laser measurements of HCHO made on the WP-3D (Wert et al., 2003; Weibring et al., 2007) allow the evaluation of the detailed plume chemistry in the model simulations with the three emission inventories (Figs. 12 and 13). The model runs with the NEI05-VOC and NEI05-VOCNOX inventories exhibit excellent agreement with the formaldehyde measurements in terms of capturing the major enhancement of formaldehyde resulting from highly reactive VOC oxidation within plumes downwind of the Houston Ship Channel. In contrast, the simulation with NEI05-REF does not predict any of the large Ship Channel HCHO plumes.

The model peaks with the NEI05-VOC and NEI05-VOCNOX do not represent the full extent of the formaldehyde plumes (Fig. 12), implying that the spatial and temporal representation of highly reactive VOC in the inventory need further improvement. Some of the HCHO peaks that the model does not capture (17:15–17:30 UTC, 18:15–18:30 UTC, 19:00–19:15 UTC) are also missing in the modeled ethylene time series; as described above, these plumes originated in the Beaumont/Port Arthur area. We expect rapid HCHO production from plumes containing elevated ethylene, and given the under-prediction of ethylene mixing ratios in these plumes, it is not surprising that the model misses the elevated HCHO here as well.

The model-simulated boundary-layer formaldehyde mixing ratios with NEI05-VOC and NEI05-VOCNOX averaged over Houston source area (see Table 4) agree with the observations within 20% for the 6 flight days examined here. The simulations with enhanced petrochemical ethylene and propylene emissions show improvement over the simulation with NEI05-REF for most of the days when the model simulations are biased low. The overall six-flight averages of the model formaldehyde with NEI05-VOCNOX (3.78 ppbv) and the observations (4.12 ppbv) over the entire Houston source area are similar (Table 10). The model bias in HCHO with NEI05-REF over the Houston Ship Channel is larger than that calculated for the whole Houston area (Fig. 13); the simulated formaldehyde with NEI05-REF over the Houston Ship Channel is about 25%–57% lower than the observations for the 6 flights. With NEI05-VOCNOX, the simulated formaldehyde over Houston Ship Channel agrees with the observations within ~30% for the same flights. On average, the model formaldehyde with NEI05-REF (3.54 ppbv) is 43% lower than the observations (6.20 ppbv) over the Houston Ship Channel (Table 10), while the 6-flight average HCHO over the region using NEI05-VOCNOX (5.12 ppbv)

is only 14% lower than the observations. Overall, the model is much better at capturing the plumes of ethylene, propylene, and formaldehyde in the Ship Channel when the updated VOC and NO_x emission inventory is used.

Figure 12 shows the time series of O₃ simulations using the NEI05-REF, the NEI05-VOC, and the NEI05-VOCNOX in comparison with the WP-3D observations for 26 September. Downwind of the Houston Ship Channel, the NOAA WP-3D aircraft observed several O₃ peaks with ~40 ppbv increases above the background. Large model-simulated O₃ differences occur among the three emission inventories coincident with the Ship Channel O₃ peaks in the airborne measurements, demonstrating the important role of NO_x and VOC emissions from industries and in-port marine vessels in the formation of O₃ in Houston. Overall, the model-simulated O₃ using NEI05-REF does not capture these observed O₃ peaks in the Ship Channel plumes, instead showing O₃ reductions of up to 20 ppbv. The model's behavior with the reference inventory in these plumes results from high NO_x emissions and moderate VOC levels, which cause net titration of O₃. The model-simulated O₃ using the NEI05-VOC is higher than that using the NEI05-REF in these plumes, with increases of up to 40 ppbv. While the increase of ethylene and propylene emissions for Ship Channel industrial sources using NEI05-VOC simulates the O₃ plumes better, the widths and peaks of the observed O₃ plumes are larger than those in the NEI05-VOC simulations because of O₃ titration within parts of these plumes. Reducing the Ship Channel NO_x emissions at the same time as ethylene and propylene emissions are increased (NEI05-VOCNOX) reduces O₃ titration and better simulates the O₃ plumes compared to the simulations with NEI05-REF and NEI05-VOC.

Figure 12 shows a number of discrepancies between the model and the observed O₃ on 26 September. Simulated O₃ using any of the inventories is generally lower than the observations everywhere, but most prominently in the regions outside the Ship Channel plumes. The observed O₃ shows a number of peaks superimposed on top of a rising background, all of which are missing in the various simulations. The causes of the observed rising O₃ background are unclear, though it appears to be the result of photochemistry. The modeled isoprene and the sum of methylvinyl ketone and methacrolein (products of isoprene oxidation) agree reasonably with the aircraft observations, indicating that missing biogenic emission is not a source of low model bias in regional O₃. As was seen with HCHO, the O₃ peaks to the east of Houston at 17:15–17:30 UTC, 18:15–18:30 UTC and 19:00–19:15 UTC (the blue arrows in Fig. 12), due to plumes originating in the Beaumont/Port Arthur area, are totally missing in the model. As with HCHO, it appears that the large underestimate of ethylene in these plumes is an indication that reactive VOC emissions for the upwind area are not correct, so it can be expected that the model will not produce adequate ozone.

Table 11. Statistics (slope and correlation coefficient r) from linear fits between observed O₃ ($=x$) and modeled O₃ ($=y$) using the NEI05-REF, NEI05-VOC and NEI05-VOCNOX inventories for the Houston area (defined in Table 4).

Date	NEI05-REF		NEI05-VOC		NEI05-VOCNOX	
	slope	r	slope	r	slope	r
9/13/2006	0.11	0.29	0.04	0.11	0.13	0.43
9/19/2006	0.36	0.61	0.41	0.76	0.47	0.90
9/25/2006	0.32	0.52	0.35	0.52	0.43	0.69
9/26/2006	-0.05	-0.10	0.13	0.26	0.35	0.56
10/5/2006	0.25	0.43	0.26	0.49	0.26	0.66
10/6/2006	0.35	0.67	0.36	0.68	0.37	0.70

Similarly, model underestimates of O₃ peaks to the west of Houston at 17:45–18:05 UTC, 18:40–18:50 UTC, and 19:30–19:45 UTC (the red arrows in Fig. 12) correspond to periods of model underestimates of HCHO, although alkene levels in this period appear to be reasonably represented. Further investigations indicate increases of observed SO₂, sulfate, CO₂, NO_y, HCHO, and O₃ to the west of Houston, implying the influence of aged power plant plumes. For example, the model SO₂ is enhanced in the inflow north and west of Houston, but the model enhancements occur farther west than those seen in the observations. This new analysis indicates that simulated power plant plumes were shifted to the west by ~ 0.5 degree longitude due to errors in transport, resulting in the low model SO₂, NO_y, HCHO, and O₃ along the actual aircraft legs west of Houston. Potential power plant sources of SO₂ plumes west of the Houston area on 26 September are Monticello, Welsh, and Martin Lake power plants north of Houston from which the plumes were transported southward during the previous day and throughout the night under a high pressure system. This extended analysis emphasizes the importance of correctly representing the influences of remote power plant sources on Houston air quality.

Low biases in modeled CO and NO_x are seen in what appear to be urban plumes detected in transects upwind of Houston on 26 September (not shown in Fig. 12). These plumes occur throughout the later transects downwind of Houston, suggesting that some of the underestimates of HCHO and O₃ might be due to an underestimate of upwind urban emissions. The inverse modeling analysis of Brioude et al. (2011) found that NEI-2005 emissions of CO and NO_x needed to be increased for suburban areas north and west of Houston, and they suggested that growth in the suburban population could have changed the spatial distribution of emissions relative to those reported in NEI-2005.

Table 11 summarizes the results of linear fits between the WP-3D O₃ ($=x$) and the model O₃ simulations ($=y$) for all boundary layer data of the 6 daytime flights within the Houston source region defined in Table 4. The slopes and correlation coefficients in the linear fits using the simulations

with the NEI05-VOC tend to improve from those with the NEI05-REF, except for 13 September 2006 when the model O₃ performance is poor, possibly because the model boundary heights are higher than the radar profiler observations (Fig. 3). The slopes and correlation coefficients in the linear fits using the simulations with NEI05-VOCNOX consistently increase from those with NEI05-VOC for all daytime flights, although the slopes are still much less than 1; the slopes range from 0.26 to 0.47 and the correlation coefficients vary from 0.56 to 0.90 with the NEI05-VOCNOX. The higher correlation coefficients of the observed O₃ with the NEI05-VOCNOX simulations points out that the large plumes resulting from the Houston industrial areas are generally captured in these flights. The low slopes of the model-observed O₃ correlations illustrate that there are sources consistently missing in even the most updated inventory investigated here.

Focusing in on just the Houston Ship Channel region, the scatter plots of observed and simulated O₃ with the 3 emission inventories for all 6 daytime flights are given in Fig. 14. From the NEI05-REF case to the NEI05-VOC case, the slope (correlation coefficient) of linear fit between the WP-3D O₃ ($=x$) and the model O₃ ($=y$) in Houston increases from 0.04 (0.05) to 0.18 (0.22). The simulated and observed O₃ are still poorly correlated when NEI05-REF and NEI05-VOC are used. From the NEI05-VOC case to the NEI05-VOCNOX case, the slope (correlation coefficient) of linear fit between the WP-3D O₃ and the model O₃ in Houston increases significantly from 0.18 (0.22) to 0.51 (0.61). Figure 14 demonstrates that the model has better capability of simulating O₃ plumes in Houston Ship Channel with the NEI05-VOCNOX compared to those with the NEI05-REF and NEI05-VOC.

5 Summary and conclusions

In this study, we evaluate the NO_x and VOC emissions in the EPA NEI-2005 in Houston, Texas during the TexAQS 2006 intensive summer campaign. Other large urban and power plant sources in Texas are also used as references for understanding emissions in the Houston-Galveston area. In the NEI-2005, major anthropogenic NO_x emissions in Houston-Galveston area originate from mobile sources, power plants, the petrochemical industry, and shipping activities, while those in other cities are mostly from mobile sources. The WRF-Chem model simulations using the NEI-2005 emissions inventory with horizontal resolutions of 20×20 km² (mother domain: continental US) and 4×4 km² (nested domain: Texas) are compared with the satellite and in-situ airborne measurements, respectively and are used to evaluate the inventory.

NO₂ columns retrieved by polar-orbiting satellite instruments (SCIAMACHY and OMI) detected strong urban and power plant plumes over Texas during the period of study. The model-simulated NO₂ columns show excellent

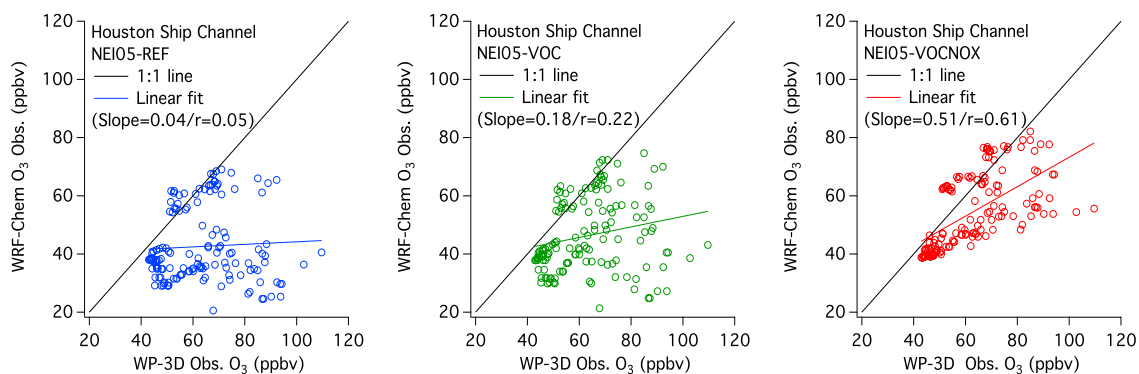


Fig. 14. Scatter plots of simulated and observed O₃ data below 1 km above ground level from 6 daytime WP-3D flights that are influenced by the sources in Houston Ship Channel. Houston Ship Channel flights are defined as in Fig. 9 for the same 6 daytime flights.

agreement with the satellite NO₂ columns for the large cities and regions with large power plants except for Houston, where the model columns are 50 %–70 % higher than the satellite columns. This study is the first in which 4 different OMI retrievals from 3 institutes are used. The 4 independent OMI NO₂ column retrievals agree within 20 % over Dallas and within 5 % over Houston.

The comparison of NOAA WP-3D NO₂ observations with the model simulations shows a similar high model bias for Houston. For the Dallas-Fort Worth plume, the model-simulated NO₂ agrees well with the WP-3D observations. For the Houston area, however, the model-simulated NO₂ with the default NEI-2005 (NEI05-REF in this study) is on average about 60 % above the observed values for the 6 daytime flights in the boundary layer over Houston. Model simulations of NO₂ mixing ratios downwind of the Houston urban core do not find significant differences with the observations, while the model overpredicts NO₂ mixing ratios by a factor of 2 in flight legs downwind of the heavily industrialized Houston Ship Channel region. The NEI05-REF total NO_x emissions in the Ship Channel are about 275 tonnes day⁻¹, which is 3 times as large as that estimated by a method using DOAS observations (Rivera et al., 2010). The largest contributor to the total NO_x in the Houston Ship Channel within NEI05-REF is the port-based ship emissions. Previous studies (Ryerson et al., 2003) also revealed the importance of industrial point source NO_x emissions in this area. The shipping emissions in the Houston Ship Channel area were studied in Williams et al. (2009) and were noted by Rivera et al. (2010), but the emissions from the ships in the port were not believed to dominate the total NO_x emissions in this area.

Industrial ethylene and propylene emissions in the NEI05-REF are greatly underestimated relative to the estimates using SOF measurements (Mellqvist et al., 2010) in the Houston Ship Channel during the period of study. When the NEI-2005 emissions of these two species are increased, by using the SOF measurements to adjust sources associated with the petrochemical industry, the model simulations of ethylene,

propylene, and formaldehyde are substantially improved in comparison with the WP-3D measurements. But remaining model-observation disagreements for these species indicate that further understanding of the spatial distribution and temporal variability of reactive VOCs is required for better model simulations. In particular, the representation of other reactive VOCs in the NEI-2005 besides ethylene and propylene in the Houston area may need to be investigated.

To examine the impact of updating both VOC and NO_x emissions on improving model-measurement agreement, we generated another modified version of NEI-2005, NEI05-VOCNOX in which the NO_x emissions across Houston Ship Channel are reduced by 70 %. Achieving these reductions in NEI-2005 NO_x emissions required the Ship Channel industrial point source emissions to be reduced by 50 % and the in-port shipping emissions in the Ship Channel to be completely omitted. The simulations with NEI05-VOCNOX gave the best overall model performance for NO₂, ethylene, propylene, HCHO, and O₃. In particular, the best simulation of O₃ in the Ship Channel required the simultaneous increase of NEI-2005 ethylene and propylene emissions from industrial activities and the reduction of NEI-2005 NO_x emissions in the Houston Ship Channel. The remaining model deficiencies in simulating WP-3D observed O₃ suggest that more effort is still required to understand the formation and transport mechanisms of O₃ in Houston.

Acknowledgements. The authors would like to thank Bryan Lambeth from the Texas Commission on Environmental Quality (TCEQ) for providing the surface observation data and the La Porte wind profiler data. The authors thank Jim Corbett and Jordan Silberman for assistance with the ship emission analysis. The authors would like to thank TCEQ for support of the evaluation of the emission inventory using satellite observations. NOAA Health of Atmosphere Program supports this study. This work is partially funded by the NOAA United States Weather Research Program through the NOAA Office of Atmospheric Research. Some of the satellite retrievals used in this study were funded by

the University of Bremen and the European Union through the ACCENT project. The Dutch-Finnish built OMI is part of the NASA EOS Aura satellite payload. The OMI project is managed by NIVR and KNMI in the Netherlands.

Edited by: R. Harley

References

- Ackermann, I. J., Hass, H., Memmesheimer, M., Ebel, A., Binkowski, F. S., and Shankar U.: Modal aerosol dynamics model for Europe: Development and first applications, *Atmos. Environ.*, 32, 2981–2999, 1998.
- Beirle, S., Platt, U., Wenig, M., and Wagner, T.: Highly resolved global distribution of tropospheric NO₂ using GOME narrow swath mode data, *Atmos. Chem. Phys.*, 4, 1913–1924, doi:10.5194/acp-4-1913-2004, 2004.
- Bishop, G. A. and Stedman, D. H.: A decade of on-road emissions measurements, *Environ. Sci. Technol.*, 42, 1651–1656, 2008.
- Boersma, K. F., Eskes, H. J., and Brinksma, E. J.: Error analysis for tropospheric NO₂ retrieval from space, *J. Geophys. Res.*, 109, D04311, doi:10.1029/2003JD003962, 2004.
- Boersma, K. F., Eskes, H. J., Veeffkind, J. P., Brinksma, E. J., van der A, R. J., Sneep, M., van den Oord, G. H. J., Levelt, P. F., Stammes, P., Gleason, J. F., and Bucsela, E. J.: Near-real time retrieval of tropospheric NO₂ from OMI, *Atmos. Chem. Phys.*, 7, 2103–2118, doi:10.5194/acp-7-2103-2007, 2007.
- Boersma, K. F., Eskes, H. J., Dirksen, R. J., van der A, R. J., Veeffkind, J. P., Stammes, P., Huijnen, V., Kleipool, Q. L., Sneep, M., Claas, J., Leitão, J., Richter, A., Zhou, Y., and Brunner, D.: An improved tropospheric NO₂ column retrieval algorithm for the Ozone Monitoring Instrument, *Atmos. Meas. Tech.*, 4, 1905–1928, doi:10.5194/amt-4-1905-2011, 2011.
- Bovensmann, J., Burrows, J. P., Buchwitz, M., Frerick, J., Noel, S., Rozanov, V. V., Chance, K. V., and Goede, A. P. H.: SCIAMACHY: Mission objectives and measurement modes, *J. Atmos. Sci.*, 56, 127–150, 1999.
- Brioude, J., Kim, S.-W., Angevine, W. M., Frost, G. J., Lee, S.-H., McKeen, S. A., Trainer, M., Fehsenfeld, F. C., Holloway, J. S., Ryerson, T. B., Williams, E. J., Petron, G., and Fast, J. D.: Top-down estimate of anthropogenic emission inventories and their interannual variability in Houston using a mesoscale inverse modeling technique, *J. Geophys. Res.*, 116, D20305, doi:10.1029/2011JD016215, 2011.
- Bucsela, E. J., Celarier, E. A., Wenig, M. O., Gleason, J. F., Veeffkind, J. P., Boersma, K. F., and Brinksma, E.: Algorithm for NO₂ vertical column retrieval from the ozone monitoring instrument, *IEEE T. Geosci. Remote Sens.*, 44, 1245–1258, doi:10.1109/TGRS.2005.863715, 2006.
- Byun, D. W., Kim, S.-T., and Kim, S.-B.: Evaluation of air quality models for the simulation of a high ozone episode in the Houston metropolitan area, *Atmos. Environ.*, 41, 837–853, 2007.
- Chen, F. and Dudhia, J.: Coupling an advanced land-surface-hydrology model with the Penn State-NCAR MM5 modeling system. Part I: Model description and implementation, *Mon. Weather Rev.*, 129, 569–585, 2001.
- Cooper, O. R., Eckhardt, S., Crawford, J. H., Brown, C. C., Cohen, R. C., Bertram, T. H., Wooldridge, P., Perring, A., Brune, W. H., Ren, X., Brunner, D., and Baughcaum, S. L.: Summer-time buildup and decay of lightning NO_x and aged thunderstorm outflow above North America, *J. Geophys. Res.*, 114, D01101, doi:10.1029/2008JD010293, 2009.
- Dallmann, T. R. and Harley, R. A.: Evaluation of mobile source emission trends in the United States, *J. Geophys. Res.*, 115, D14305, doi:10.1029/2010JD013862, 2010.
- De Gouw, J. A., Te Lintel Hekkert, S., Mellqvist, J., Warneke, C., Atlas, E. L., Fehsenfeld, F. C., Fried, A., Frost, G. J., Harren, F. J. M., Holloway, J. S., Lefer, B., Lueb, R., Meagher, J. F., Parrish, D. D., Patel, M., Pope, L., Richter, D., Rivera, C., Ryerson, T. B., Samuelsson, J., Walega, J., Washenfelder, R. A., Weibring, P., and Zhu, X.: Airborne measurements of ethane from industrial sources using laser photo-acoustic spectroscopy, *Environ. Sci. Technol.*, 43, 2437–2442, 2009.
- Dyer, A. J. and Hicks, B. B.: Flux-gradient relationships in the constant flux layer, *Q. J. Roy. Meteor. Soc.*, 96, 715–721, 1970.
- Gilman, J. B., Kuster, W. C., Goldan, P. D., Herndon, S. C., Zahniser, M. S., Tucker, S. C., Brewer, W. A., Lerner, B. M., Williams, E. J., Harley, R. A., Fehsenfeld, F. C., Warneke, C., and de Gouw, J. A.: Measurements of volatile organic compounds during the 2006 TexAQS/GoMACCS campaign: Industrial influences, regional characteristics, and diurnal dependencies of the OH reactivity, *J. Geophys. Res.*, 114, D00F06, doi:10.1029/2008JD011525, 2009.
- Grell, G. A. and Devenyi, D.: A generalized approach to parameterizing convection combining ensemble and data assimilation techniques, *Geophys. Res. Lett.*, 29, 1693, doi:10.1029/2002GL015311, 2002.
- Grell, G. A., Peckham, S. E., Schmitz, R., McKeen, S. A., Frost, G., Skamarock, W., and Eder, B.: Fully coupled 'online' chemistry within the WRF model, *Atmos. Environ.*, 39, 6957–6975, 2005.
- Haagen-Smit, A. J.: Chemistry and physiology of Los Angeles smog, *Ind. Eng. Chem.*, 44, 1342–1346, 1952.
- Heckel, A., Kim, S.-W., Frost, G. J., Richter, A., Trainer, M., and Burrows, J. P.: Influence of low spatial resolution a priori data on tropospheric NO₂ satellite retrievals, *Atmos. Meas. Tech.*, 4, 1805–1820, doi:10.5194/amt-4-1805-2011, 2011.
- Hong, S.-Y., Noh, Y., and Dudhia, J.: A new vertical diffusion package with an explicit treatment of entrainment processes, *Mon. Weather Rev.*, 134, 2318–2341, doi:10.1175/MWR3199.1, 2006.
- Huijnen, V., Eskes, H. J., Poupkou, A., Elbern, H., Boersma, K. F., Foret, G., Sofiev, M., Valdebenito, A., Flemming, J., Stein, O., Gross, A., Robertson, L., D'Isidoro, M., Kioutsioukis, I., Friese, E., Amstrup, B., Bergstrom, R., Strunk, A., Vira, J., Zyryanov, D., Maurizi, A., Melas, D., Peuch, V.-H., and Zerefos, C.: Comparison of OMI NO₂ tropospheric columns with an ensemble of global and European regional air quality models, *Atmos. Chem. Phys.*, 10, 3273–3296, doi:10.5194/acp-10-3273-2010, 2010.
- Jiang, G. and Fast, J. D.: Modeling the effects of VOC and NO_x emission sources on ozone formation in Houston during the TexAQS 2000 field campaign, *Atmos. Environ.*, 38, 5071–5085, 2004.
- Jobson, B. T., Berkowitz, C. M., Kuster, W. C., Goldan, P. D., Williams, E. J., Fehsenfeld, F. C., Apel, E. C., Karl, T., Lonnenman, W. A., and Riemer, D.: Hydrocarbon source signatures in Houston, Texas: Influence of the petrochemical industry, *J. Geophys. Res.*, 109, D24305, doi:10.1029/2004JD004887, 2004.

- Kim, E., Brown, S. G., Hafner, H. R., and Hopke, P. K.: Characterization of non-methane volatile organic compounds sources in Houston during 2001 using positive matrix factorization, *Atmos. Environ.*, 39, 5934–5946, 2005.
- Kim, S.-W., Heckel, A., McKeen, S. A., Frost, G., Hsie, E.-Y., Trainer, M. K., Richter, A., Burrows, J. P., Peckham, S. E., and Grell, G. A.: Satellite-observed U.S. power plant NO_x emission reductions and their impact on air quality, *Geophys. Res. Lett.*, 33, L22812, doi:10.1029/2006GL027749, 2006.
- Kim, S.-W., Heckel, A., Frost, G. J., Richter, A., Gleason, J., Burrows, J. P., McKeen, S., Hsie, E.-Y., Granier, C., and Trainer, M.: NO₂ columns in the western United States observed from space and simulated by a regional chemistry model and their implications for NO_x emissions, *J. Geophys. Res.*, 114, D11301, doi:10.1029/2008JD011343, 2009.
- Kleinman, L. I., Daum, P. H., Imre, D., Lee, Y.-N., Nunnermacker, L. J., Springston, S. R., Weinstein-Lloyd, J., and Rudolph, J.: Ozone production rate and hydrocarbon reactivity in 5 urban areas: A cause of high ozone concentration in Houston, *Geophys. Res. Lett.*, 29, 1467, doi:10.1029/2001GL014569, 2002.
- Konovalov, I. B., Beekmann, M., Richter, A., and Burrows, J. P.: Inverse modelling of the spatial distribution of NO_x emissions on a continental scale using satellite data, *Atmos. Chem. Phys.*, 6, 1747–1770, doi:10.5194/acp-6-1747-2006, 2006.
- Lamsal, L. N., Martin, R. V., van Donkelaar, A., Celarier, E. A., Bucsela, E. J., Boersma, K. F., Dirksen, R., Luo, C., and Wang, Y.: Indirect validation of tropospheric nitrogen dioxide retrieved from the OMI satellite instrument: Insight into the seasonal variation of nitrogen oxides at northern midlatitudes, *J. Geophys. Res.*, 115, D05302, doi:10.1029/2009JD013351, 2010.
- Lee, S.-H., Kim, S.-W., Angevine, W. M., Bianco, L., McKeen, S. A., Senff, C. J., Trainer, M., Tucker, S. C., and Zamora, R. J.: Evaluation of urban surface parameterizations in the WRF model using measurements during the Texas Air Quality Study 2006 field campaign, *Atmos. Chem. Phys.*, 11, 2127–2143, doi:10.5194/acp-11-2127-2011, 2011a.
- Lee, S.-H., Kim, S.-W., Trainer, M., Frost, G. J., McKeen, S. A., Cooper, O. R., Flocke, F., Holloway, J. S., Neuman, J. A., Ryerson, T., Senff, C. J., Swanson, A. L., and Thompson, A. M.: Modeling ozone plumes observed downwind of New York City over the North Atlantic Ocean during the ICARTT field campaign, *Atmos. Chem. Phys.*, 11, 7375–7397, doi:10.5194/acp-11-7375-2011, 2011b.
- Levelt, P. F., van den Oord, G. H. J., Dobber, M. R., Malkki, A., Visser, H., de Vries, J., Stammes, P., Lundell, J., and Saari, H.: The ozone monitoring instrument, *IEEE T. Geosci. Remote Sens.*, 44, 1093–1101, doi:10.1109/TGRS.2006.872333, 2006.
- Lin, Y.-L., Farley, R. D., and Orville, H. D.: Bulk parameterization of the snow field in a cloud model, *J. Climate Appl. Meteor.*, 22, 1065–1092, 1983.
- Madronich, S.: Photodissociation in the atmosphere: 1. Actinic flux and the effects of ground reflections and clouds, *J. Geophys. Res.*, 92, 9740–9752, doi:10.1029/JD092iD08p09740, 1987.
- Martin, R. V., Jacob, D. J., Chance, K., Kurosu, T. P., Palmer, P. I., and Evans, M. J.: Global inventory of nitrogen oxides emissions constrained by space-based observations of NO₂ columns, *J. Geophys. Res.*, 108, 4537, doi:10.1029/2003JD003453, 2003.
- McCoy, B. J., Fischbeck, P. S., and Gerard, D.: How big is big? How often is often? Characterizing Texas petroleum refining up-set air emissions, *Atmos. Environ.*, 44, 4230–4239, 2010.
- McKeen, S., Grell, G., Peckham, S., Wilczak, J., Djalalova, I., Hsie, E.-Y., Frost, G., Peischl, J., Schwarz, J., Spackman, R., Holloway, J., de Gouw, J., Warneke, C., Gong, W., Bouchet, V., Gaudreault, S., Racine, J., McHenry, J., McQueen, J., Lee, P., Tang, Y., Carmichael, G. R., and Mathur, R.: An evaluation of real-time air quality forecasts and their urban emissions over eastern Texas during the summer of 2006 Second Texas Air Quality Study field study, *J. Geophys. Res.*, 114, D00F11, doi:10.1029/2008JD011697, 2009.
- Mellqvist, J., Samuelsson, J., Johansson, J., Rivera, C., Lefter, B., Alvarez, S., and Jolly, J.: Measurements of industrial emissions of alkenes in Texas using the solar occultation flux method, *J. Geophys. Res.*, 115 D00F17, doi:10.1029/2008JD011682, 2010.
- Mlawer, E. J., Taubman, S. J., Brown, P. D., Iacono, M. J., and Clough, S. A.: Radiative transfer for inhomogeneous atmosphere: RRTM, a validated correlated-k model for the long-wave, *J. Geophys. Res.*, 102, 16663–16682, doi:10.1029/97JD00237, 1997.
- Murphy, C. F. and Allen, D. T.: Hydrocarbon emissions from industrial release events in the Houston-Galveston area and their impact on ozone formation, *Atmos. Environ.*, 39, 3785–3798, 2005.
- Nam, J., Kimura, Y., Vizuete, W., Murphy, C., and Allen, D. T.: Modeling the impacts of emission events on ozone formation in Houston, Texas, *Atmos. Environ.*, 40, 5329–5341, 2006.
- National Aeronautics and Space Administration: OMI Algorithm Theoretical Basis Document, Volume IV – OMI Trace Gas Algorithms, edited by: Chance, K., ATBD-OMI-04, Version 2.0, August 2002, available at: http://eosps.gsf.nasa.gov/eos_homepage/for_scientists/atbd/viewInstrument.php?instrument=13, 2002.
- Parrish, D. D., Allen, D. T., Bates, T. S., Estes, M., Fehsenfeld, F. C., Feingold, G., Ferrare, R., Hardesty, R. M., Meagher, J. F., Nielsen-Gammon, J. W., Pierce, R. B., Ryerson, T. B., Seinfeld, J. H., and Williams, E. J.: Overview of the Second Texas Air Quality Study (TexAQS II) and the Gulf of Mexico Atmospheric Composition and Climate Study (GoMACCS), *J. Geophys. Res.*, 114, D00F13, doi:10.1029/2009JD011842, 2009.
- Paulson, C. A.: The mathematical representation of wind speed and temperature profiles in the unstable atmospheric surface layer, *J. Appl. Meteor.*, 9, 857–861, 1970.
- Peischl, J., Ryerson, T. B., Holloway, J. S., Parrish, D. D., Trainer, M., Frost, G. J., Aikin, K. C., Brown, S. S., Dubé, W. P., Stark, H., and Fehsenfeld, F. C.: A top-down analysis of emissions from selected Texas power plants during TexAQS 2000 and 2006, *J. Geophys. Res.*, 115, D16303, doi:10.1029/2009JD013527, 2010.
- Richter, A. and Burrows, J. P.: Tropospheric NO₂ from GOME measurements, *Adv. Space Res.*, 29, 1673–1683, 2002.
- Richter, A., Burrows, J. P., Nub, H., Granier, C., and Niemeier, U.: Increase in tropospheric nitrogen dioxide levels over China observed from space, *Nature*, 437, 129–132, 2005.
- Rivera, C., Mellqvist, J., Samuelsson, J., Lefter, B., Alvarez, S., and Patel, M. R.: Quantification of NO₂ and SO₂ emissions from the Houston Ship Channel and Texas City industrial areas during the 2006 Texas Air Quality Study, *J. Geophys. Res.*, 115 D08301, doi:10.1029/2009JD012675, 2010.
- Russell, A. R., Valin, L. C., Bucsela, E. J., Wenig, M. O., and Cohen, R. C.: Space-based constraints on spatial and temporal pat-

- terns of NO_x emissions in California, 2005–2008, *Environ. Sci. Technol.*, 44, 3608–3615, 2010.
- Ryerson, T. B., Buhr, M. P., Frost, G. J., Goldan, P. D., Holloway, J. S., Hubler, G., Jobson, B. T., Kuster, W. C., McKeen, S. A., Parrish, D. D., Roberts, J. M., Sueper, D. T., Trainer, M., Williams, J., and Fehsenfeld, F. C.: Emissions lifetimes and ozone formation in power plant plumes, *J. Geophys. Res.*, 103, 22569–22583, 1998.
- Ryerson, T. B., Trainer, M., Angevine, W. M., Brock, C. A., Dissly, R. W., Fehsenfeld, F. C., Frost, G. J., Goldan, P. D., Holloway, J. S., Hubler, G., Jakoubek, R. O., Kuster, W. C., Neuman, J. A., Nicks Jr., D. K., Parrish, D. D., Roberts, J. M., and Sueper, D. T.: Effect of petrochemical industrial emissions of reactive alkenes and NO_x on tropospheric ozone formation in Houston, Texas, *J. Geophys. Res.*, 108 D084249, doi:10.1029/2002JD003070, 2003.
- Schauffler, S. M., Atlas, E. L., Blake, D. R., Flocke, F., Lueb, R. A., Lee-Taylor, J. M., Stroud, V., and Travniccek, W.: Distributions of brominated organic compounds in the troposphere and lower stratosphere, *J. Geophys. Res.*, 104, 21513–21535, doi:10.1029/1999JD900197, 1999.
- Schauffler, S. M., Atlas, E. L., Donnelly, S. G., Andrews, A., Montzka, S. A., Elkins, J. W., Hurst, D. F., Romashkin, P. A., Dutton, G. S., and Stroud, V.: Chlorine budget and partitioning during the Stratospheric Aerosol and Gas Experiment (SAGE) III Ozone Loss and Validation Experiment (SOLVE), *J. Geophys. Res.*, 108, 4173, doi:10.1029/2001JD002040, 2003.
- Schell, B., Ackermann, I. J., Hass, H., Binkowski, F. S., and Ebel, A.: Modeling the formation of secondary organic aerosol within a comprehensive air quality model system, *J. Geophys. Res.*, 106, 28275–28293, doi:10.1029/2001JD000384, 2001.
- SIAM, LAPACK Users' Guide, 3rd ed., SIAM Publications, Philadelphia, 1999.
- Skamarock, W. C., Klemp, J. B., Dudhia, J., Gill, D. O., Barker, D. M., Duda, M. G., Hwang, X.-Y., Wang, W., and Powers, J. G.: A description of the advanced research WRF version 3, Technical Note 475+STR, National Center for Atmospheric Research, Boulder, CO, USA, 2008.
- US Environmental Protection Agency, 2005: EPA's National Mobile Inventory Model (NMIM), A Consolidated Emissions Modeling System for MOBILE6 and NONROAD, EPA420-R-05-024, 24 pp., Washington, DC, available at: <http://www.epa.gov/otaq/models/nmim/420r05024.pdf>, 2005.
- US Environmental Protection Agency, 2007: Commercial Marine Port Inventory Development 2002 and 2005, Appendix A for EPA420-D-07-007, Inventories Assessment and Standards Division Office of Transportation and Air Quality U.S. Environmental Protection Agency, Prepared for EPA by ICF International San Francisco, CA, EPA Contract No. EP-C-06-094 Work Assignment No. 0-02, available at: ftp://ftp.epa.gov/EmisInventory/2005_nei/mobile/commercial_marine_vessels_2002_and_2005.pdf, 2007.
- US Environmental Protection Agency, 2008: Technical Support Document: Preparation of Emissions Inventories for the 2002-based Platform, Version 3, Criteria Air Pollutants, 77 pp., Office of Air Quality Planning and Standards, Air Quality Assessment Division, available at: www.epa.gov/scram001/reports/Emissions%20TSD%20Vol1_02-28-08.pdf, 2008.
- US Environmental Protection Agency, 2010: Technical Support Document: Preparation of Emissions Inventories for the Version 4, 2005-based Platform, 73 pp., Office of Air Quality Planning and Standards, Air Quality Assessment Division, available at: http://www.epa.gov/airquality/transport/pdfs/2005-emissions_tsd_07jul2010.pdf, 2010.
- van der A, R. J., Eskes, H. J., Boersma, K. F., van Noije, T. P. C., Van Roozendaal, M., De Smedt, I., Peters, D. H. M. U., and Meijer, E. W.: Trends, seasonal variability and dominant NO_x source derived from a ten year record of NO₂ measured from space, *J. Geophys. Res.*, 113, D04302, doi:10.1029/2007JD009021, 2008.
- van Noije, T. P. C., Eskes, H. J., Dentener, F. J., Stevenson, D. S., Ellingsen, K., Schultz, M. G., Wild, O., Amann, M., Atherton, C. S., Bergmann, D. J., Bey, I., Boersma, K. F., Butler, T., Co-fala, J., Drevet, J., Fiore, A. M., Gauss, M., Hauglustaine, D. A., Horowitz, L. W., Isaksen, I. S. A., Krol, M. C., Lamarque, J.-F., Lawrence, M. G., Martin, R. V., Montanaro, V., Müller, J.-F., Pitari, G., Prather, M. J., Pyle, J. A., Richter, A., Rodriguez, J. M., Savage, N. H., Strahan, S. E., Sudo, K., Szopa, S., and van Roozendaal, M.: Multi-model ensemble simulations of tropospheric NO₂ compared with GOME retrievals for the year 2000, *Atmos. Chem. Phys.*, 6, 2943–2979, doi:10.5194/acp-6-2943-2006, 2006.
- Vizuete, W., Kim, B.-U., Jeffries, H., Kimura, Y., Allen, D. T., Kioumourtoglou, M.-A., Biton, L., and Henderson, B.: Modeling ozone formation from industrial emission events in Houston, Texas, *Atmos. Environ.*, 42, 7641–7650, 2008.
- Wang, H., Skamarock, W. C., and Feingold, G.: Evaluation of scalar advection schemes in the Advanced Research WRF model using large-eddy simulations of aerosol–cloud interactions, *Mon. Weather Rev.*, 137, 2547–2558, 2009.
- Washenfelder, R. A., Trainer, M., Frost, G. J., Ryerson, T. B., Atlas, E. L., de Gouw, J. A., Flocke, F. M., Fried, A., Holloway, J. S., Parrish, D. D., Peischl, J., Richter, D., Schauffler, S. M., Walega, J. G., Warneke, C., Weibring, P., and Zheng, W.: Characterization of NO_x, SO₂, ethane, and propene from industrial emission sources in Houston, Texas, *J. Geophys. Res.*, 115, D16311, doi:10.1029/2009JD013645, 2010.
- Webster, M., Nam, J., Kimura, Y., Jeffries, H., Vizuete, W., and Allen, D. T.: The effect of variability in industrial emissions on ozone formation in Houston, Texas, *Atmos. Environ.*, 41, 9580–9593, 2007.
- Weibring, P., Richter, D., Walega, J. G., and Fried, A.: First demonstration of a high performance difference frequency spectrometer on airborne platforms, *Opt. Express*, 15, 13476–13495, 2007.
- Wert, B. P., Trainer, M., Fried, A., Ryerson, T. B., Henry, B., Potter, W., Angevine, W. M., Atlas, E., Donnelly, S. G., Fehsenfeld, F. C., Frost, G. J., Goldan, P. D., Hansel, A., Holloway, J. S., Hubler, G., Kuster, W. C., Nicks Jr., D. K., Neuman, J. A., Parrish, D. D., Schauffler, S., Stutz, J., Sueper, D. T., Wiedinmyer, C., Wisthaler, A., Signatures of terminal alkene oxidation in airborne formaldehyde measurements during TexAQS 2000, *J. Geophys. Res.*, 108, 4104, doi:10.1029/2002JD002502, 2003.
- Williams, E. J., Lerner, B. M., Murphy, P. C., Herndon, S. C., and Zahniser, M. S.: Emissions of NO_x, SO₂, CO, and HCHO from commercial marine shipping during Texas Air Quality Study (TexAQS) 2006, *J. Geophys. Res.*, 114, D21306, doi:10.1029/2009JD012094, 2009.

Zhang, R., Lei, W., Tie, X., and Hess, P.: Industrial emissions cause extreme urban ozone diurnal variability, *P. Natl. Acad. Sci. USA*, 101, 6346–6350, 2004.

Zhang, Q., Streets, D. G., and He, K.: Satellite observations of recent power plant construction in Inner Mongolia, China, *Geophys. Res. Lett.*, 36, L15809, doi:10.1029/2009GL038984, 2009.